Inverse problems for nonlinear equations: direct and iterative methods

Maxim Shishlenin

Sergey Kabanikhin, Nikita Novikov, Dmitry Klyuchinsky, Nikita Savchenko, Maxim Dudar

Sobolev Institute of Mathematics

Institute of Computational Mathematics and Mathematical Geophysics

Novosibirsk State University

Dynamics in Siberia
Sobolev Institute of Mathematics
March 2 – 6, 2026

Motivation

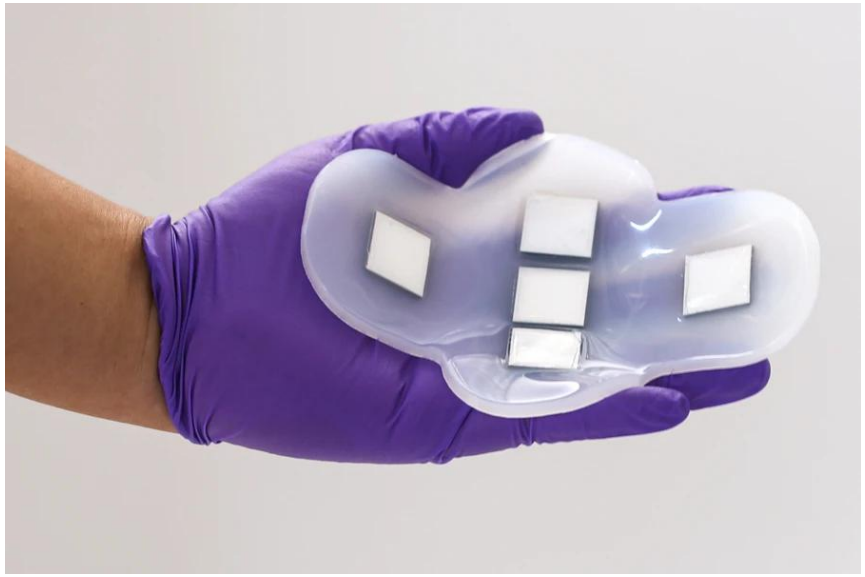

The wearable ultrasound patch (cUSB-Patch) is developed by researchers at the Massachusetts Institute of Technology (MIT).

Purpose: The device was originally designed for non-invasive monitoring of bladder fullness. It helps patients with kidney or bladder diseases to monitor the functioning of these organs without visiting a clinic.

Design: The device is a flexible silicone rubber patch with five ultrasonic arrays embedded in it. The matrices are arranged in the shape of the letter "X", which provides a wide field of view.

Advantages: Gel-free technology: Unlike traditional ultrasound, this patch does not require the use of cold gel to transmit a signal.

Autonomy: Patients can use it independently at home without the help of an operator.

Versatility: The researchers believe that the technology can be adapted for imaging other internal organs and early diagnosis of tumors located deep in the body.

The accuracy of determining the volume of the bladder using this patch is comparable to the results of traditional ultrasound devices.

Motivation

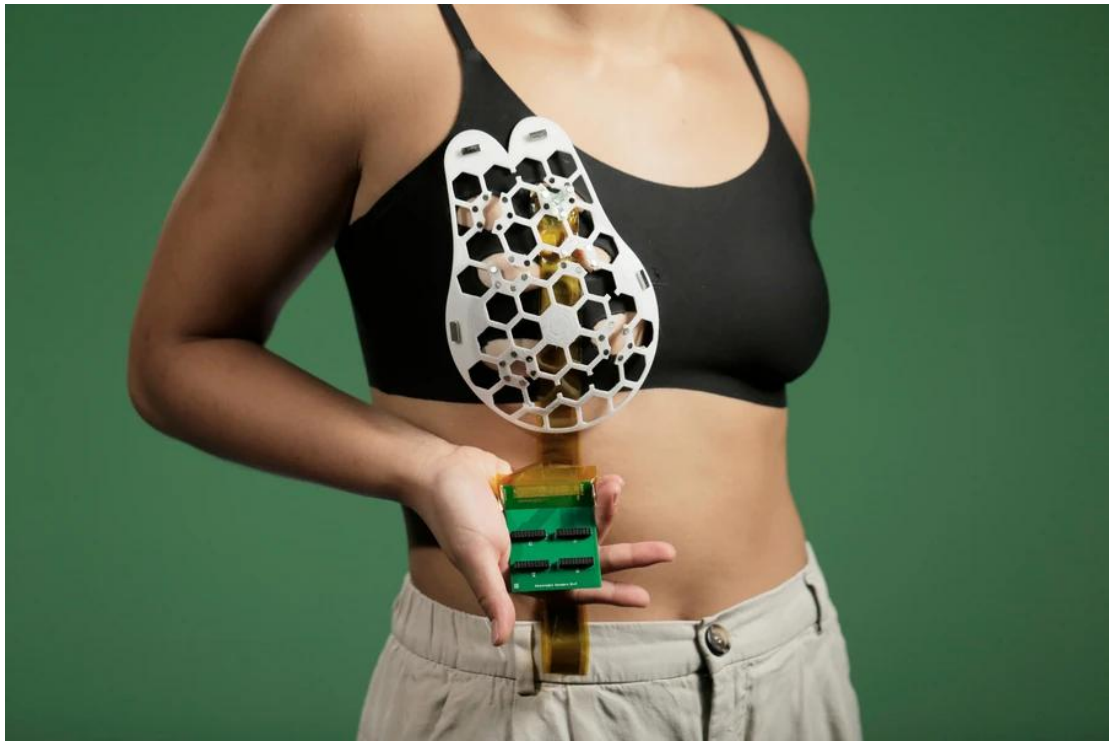

Ultrasound allows real-time imaging of deeply located tissues, organs, and blood flow in a safe and non-invasive manner. This is the most widely used method of medical imaging in terms of the number of images created annually. Where modern ultrasound systems require guidance and positioning by a sonographer, flexible and oversized ultrasound arrays provide hands-free imaging and are a solution for short- and long-term monitoring.

The wearable ultrasound device for early detection of breast cancer (MIT).

Technology: The device uses ultrasound, similar to that used in medical centers, but designed as a flexible patch.

Application: For use by at-risk patients at home or between scheduled mammograms.

Features: Flexible 3D-printed frame allows the ultrasound scanner to move over the surface of the breast, providing high-quality visualization.

Purpose: Helps to detect tumors at an early stage, which improves survival.

Motivation

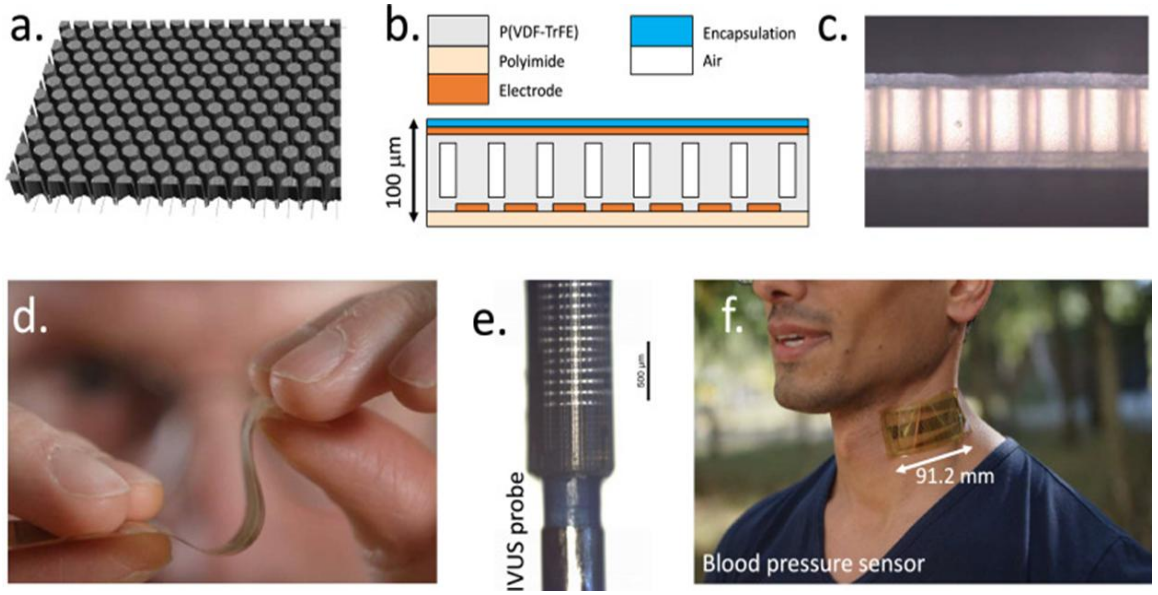

Технология PillarWave™ — гибкие ультразвуковые датчики на основе пьезоэлектрического полимера P(VDF-TrFE). Эта разработка, опубликованная в журнале Nature Communications в 2024 году, позволяет создавать тонкие и растяжимые сенсоры для медицинского мониторинга.

van Neer P.L.M.J., Peters L.C.J.M., Verbeek R.G.F.A. *et al.* Flexible large-area ultrasound arrays for medical applications made using embossed polymer structures. *Nat Commun* **15**, 2802 (2024).

Материал: Основным компонентом является сополимер P(VDF-TrFE), обладающий пьезоэлектрическими свойствами.
Конструкция: С помощью термотиснения на полимерной пленке создается массив «столбиков» (пилларов), окруженных воздухом. Это придает датчику высокую гибкость и улучшает его акустические характеристики.
Толщина: Общая толщина устройства составляет всего 100 мкм (0,1 мм), что делает его почти неощутимым на коже.
Применение
Гибкость (d): Датчик может изгибаться с радиусом менее 1 мм без потери функциональности.
Внутрисосудистое УЗИ (e): Благодаря своей тонкости сенсор можно обернуть вокруг наконечника катетера диаметром менее 1 мм для визуализации стенок сосудов изнутри.
Мониторинг давления (f): На фото показан пластырь размером 91,2 мм, закрепленный на шее. Он использует ультразвуковые волны для непрерывного и неинвазивного отслеживания диаметра сонной артерии, что позволяет точно измерять артериальное давление в реальном времени без использования манжеты.

Motivation

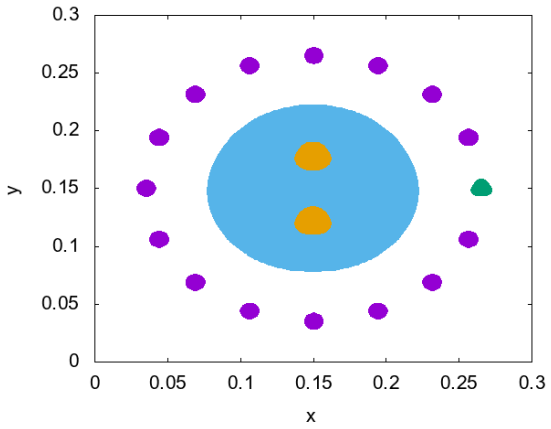

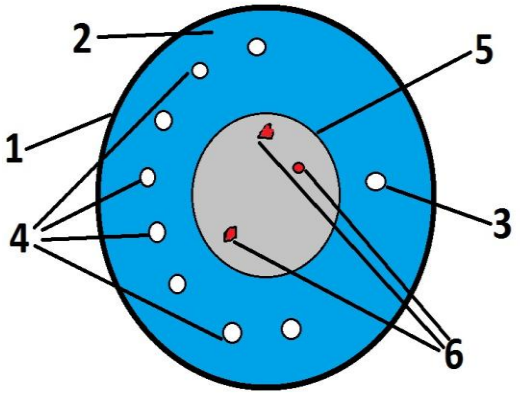

1 – The boundary of the tomograph;
2 – Filler (water);
3 – The source of the probing signal;
4 – Acoustic wave receivers;
5 – The object of the study;
6 – Inclusions inside the object

January 29, 2025. Moscow State University - acoustic tomograph prototype. Olga Rumyantseva, Andrey Shurup, Konstantin Dmitriev, Dmitry Zotov, M.Sh.

Aim: To develop methods and algorithms for the early detection of tumors in human soft tissues and to test them on real data.

Project: Interdisciplinary project RSF 25-61-00027
"Wave tomography: supercomputer modeling, machine learning and experiment"
Co-executors: Sobolev Institute of Mathematics, Institute of Computational Mathematics and Mathematical Geophysics, Moscow State University and
All-Russian Scientific Research Institute of Experimental Physics (Sarov):

3D digital twin + prototype of a medical acoustic tomograph

Introduction

Hyperbolic system of equations:
- Conservation laws.
- Piecewise smooth media.
- Inverse problem - the boundaries are unknown.

Tomograph parameters: Probe pulse: average frequency 1.25 MHz, bandwidth 300 kHz, pulse duration 12 microseconds. Pulse shape: the envelope first increases, then peaks and falls.

Resolution: theoretically about 0.3-0.5 mm in the tomography plane (about one third of the characteristic wavelength).

In the direction perpendicular to the tomography plane, it is still about 1-1.5 cm (thickness of the studied layer) due to the height of the transducers; however, additional measures can improve the vertical resolution by at least 5 times.

A phantom is placed in the water, with the acoustic parameters are close to the human body.

Human body acoustic parameters

Golubinsky A. N., Dvoryankin S. V. On the issue of parameterization of the results of acoustic sensing of the human body (frequency response) in the implementation of the contact-difference method of audio identification. Special equipment and communications. 2011. 2.
T. D. Mast. Empirical relationships between acoustic parameters in human soft tissues. Acoustics Research Letters. 2000. 1.
S. A. Goss, R. L. Johnston, F. Dunn. Comprehensive compilation of empirical ultrasonic properties of mammalian tissues. J. Acoustical Society of America. 1978. 64.

Introduction

One of the main problems of ultrasound tomography is the development of methods for solving nonlinear inverse problems. The most suitable model is a 3d inverse problem in which the wave propagation velocity, density and attenuation are reconstructed from the data recorded by detectors located at the boundary of the studied region.

Inverse problems of wave tomography and geometric optics have been investigated in [Huang et al. 2007; Glide et al. 2008; Natterer 2011; Jirik et al. 2012, Novikov, Grinevich; Novikov; Wiskin et al. 2013, 2017, 2019, Klibanov et al. 1995, 1997, 2019, 2025].

The following approaches have been applied to restoring the speed of sound, based on

- **Kirchhoff migration** [Duric et al. 2012,2024],
- **Image processing** [Jirik et al. 2012],
- **Helmholtz equation** [Wiskin et al. 2013, 2017; Bakushinsky, Leonov, 2019, 2020],
- **Wave equation of the 2nd order** [Zhao et al 2022; Gemmeke et al 2017-2025; Lucka et al 2021, 2023; Goncharsky et al. 2014, 2017],
- **Reverse time migration** [Filatova et al. 2016, 2018],
- **NN** [Li et al. 2019, Fan et al. 2022; Basurto-Hurtado et al 2022; Zhang et al. 2023]
- **Bayesian method** [Yin et al. 2023]

Motivation

Delphinus Medical Technologies → QT Imaging

N. Duric, Co-Founder And Chief Technology Officer
P.J. Littrup, Co-Founder And Medical Advisor

→ Inverse tomography problems in the frequency domain + AI

Our advantages: combined inverse problems: **dynamic**, **kinematic** and frequency domain + **AI**.

2.5D tomography in the frequency domain (gluing thin layers)

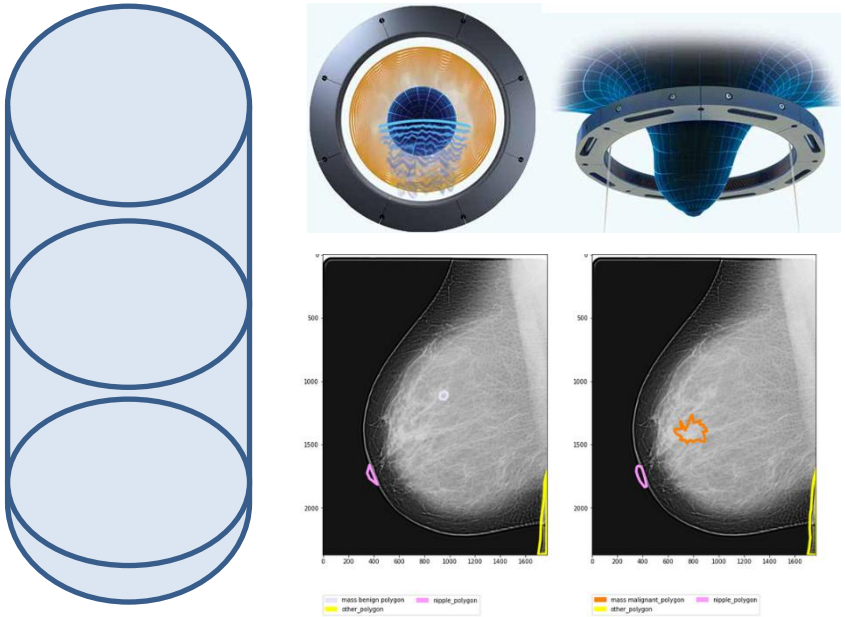

https://www.delphinusmt.com/technology/

3D tomography in the frequency domain

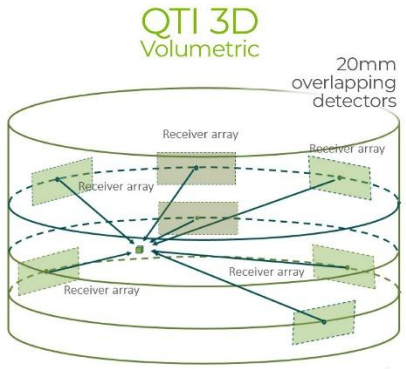

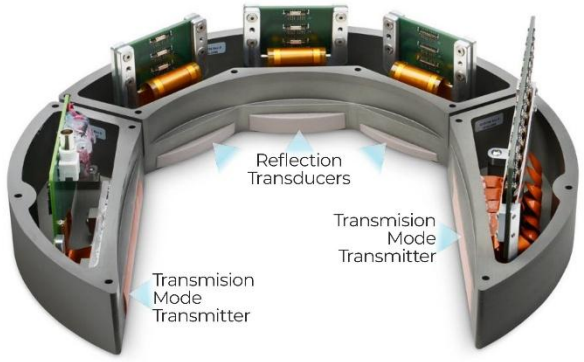

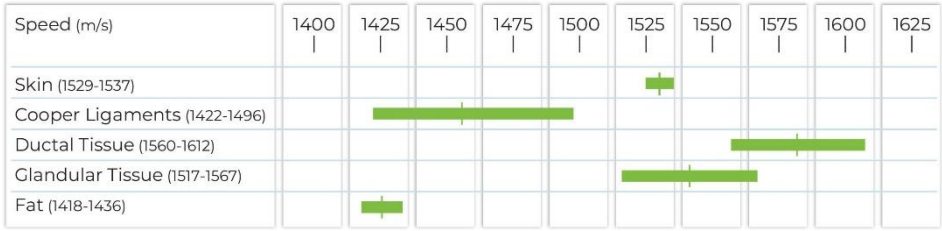

https://www.qtimaging.com/image-reconstruction-algorithms/

Motivation

The development of direct methods for solving inverse problems is a very urgent problem in specific applications.

The main idea is to reduce discrete inverse problems to system of linear algebraic equations with poorly conditioned (or degenerate) matrices of gigantic dimension.

Methods:

- Gelfnd-Levitan-Krein method: the nonlinear inverse problem is reduced to the system of linear integral equations.
- Method of lines: using spatial approximation, we get the ODE system, which is solved by the matrix method.

We apply the low–rank approximation for system of linear algebraic equations to solve an applied inverse problem in real time for arbitrary data.

Applications:

- **geophysics (earthquake sources, microseismic monitoring);**
- **medical acoustic tomography;**
- **marine acoustics (internal waves, tsunami waves, etc.).**

3D M.G. Krein method

$$c^{-2}(z)u_{tt}^{(k)} = \Delta u^{(k)} - \nabla \ln \rho\,(z,y)\nabla u^{(k)}, \qquad z > 0, y \in R^2, t > 0, k = (k_1, k_2) \in Z^2,$$
$$u^{(k)}|_{t<0} \equiv 0,$$
$$u_z^{(k)}(+0, y, t) = \delta(y - y^{(0)})\delta(t)$$

Inverse problem: find $\rho(x,y)$ or $c(z)$ using additional information at the plane $z = 0$

$$u^{(k)}(+0, y, t) = f^{(k)}(y, t; y^{(0)})$$

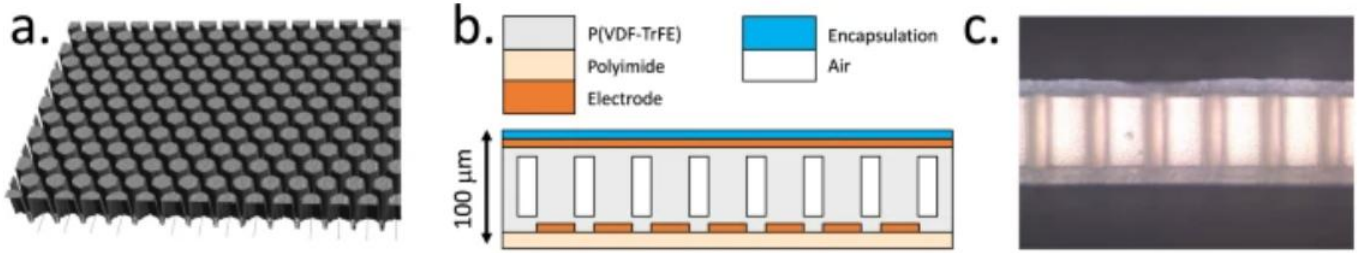

All functions are supposed to be 2π-periodic with respect to y_1 and y_2, i.e.

$$f^{(k)}(y,t) = \sum_m f_m^{(k)}(t)e^{i(m,y)}$$

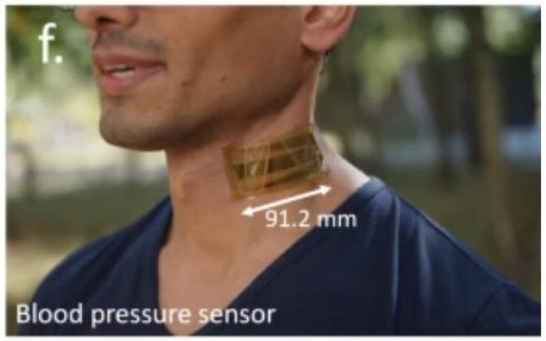

S.I. Kabanikhin. On linear regularization of multidimensional inverse problems for hyperbolic equations. Doklady RAS. Vol. 309, No. 4 (1989).
Kabanikhin S.I., Satybaev A.D., Shishlenin M.A. Direct methods of solving inverse hyperbolic problems. VSP/BRILL, the Netherlands, 2004.

Krein equation

New variable $x = \int_0^z \frac{d\xi}{c(\xi)}$

$$u_{tt}^{(k)} = \sigma(x,y)\left[\frac{\partial}{\partial x}\left(\frac{u_x^{(k)}}{\sigma}\right) + c^2(x)\frac{\partial}{\partial y}\left(\frac{u_y^{(k)}}{\sigma}\right)\right];$$

Here $\sigma(x,y) = c(x)\rho(x,y)$

$$u^{(k)}|_{t<0} \equiv 0, x > 0, y \in (-\pi,\pi);$$

$$u^{(k)}|_{y=-\pi} = u^{(k)}|_{y=\pi};$$

$$u_x^{(k)}|_{x=0} = c_0 e^{iky}\delta(t), t > 0, y \in \mathbb{R}.$$

$$u^{(k)}(+0,y,t) = f^{(k)}(y,t), t > 0, y \in \mathbb{R}$$

$$\Phi^{(k)}(x,t) - \frac{1}{2c_0}\sum_{m\in\mathbb{Z}}\int_{-x}^{x} f_m^{(k)\prime}(t-s)\Phi^{(m)}(x,s)ds = \frac{1}{2c_0}\int_{-\pi}^{\pi}\frac{e^{iky}}{\rho(0,y)}dy.$$

$$\sigma(x,y) = \frac{\pi^2}{\rho(0,y)}\Big[\sum_{m\in\mathbb{Z}}\Phi^{(m)}(x,x-0)e^{-imy}\Big]^{-2}$$

Gelfand-Levitan equation

New function

$$u(x,y,t) = c_0\sqrt{\frac{\sigma(x,y)}{\sigma(0,y)}}v(x,y,t).$$

$$v_{tt} = \Delta_{x,y}v(x,y,t) + q(x,y)v;$$
$$x > 0, \quad y \in (-\pi,\pi), \quad t > 0,$$
$$v^{(k)}|_{t<0} \equiv 0,$$
$$v_x^{(k)}|_{x=0} = \delta(t)e^{iky}.$$

Here $$q(x,y) = \left[\frac{1}{2}\left(\frac{\sigma_x}{\sigma}\right)_x - \frac{1}{4}\left(\frac{\sigma_x}{\sigma}\right)^2\right] + c^2(x)\left[\frac{1}{2}\left(\frac{\sigma_y}{\sigma}\right)_y - \frac{1}{4}\left(\frac{\sigma_y}{\sigma}\right)^2\right].$$

$$c_0 w^{(k)}(x,y,t) + \int_{-x}^{x}\sum_{m\in\mathbb{Z}} f_m^{(k)\prime}(t-s)w^{(m)}(x,y,s)ds =$$

$$= -\frac{1}{2}\left[f^{(k)\prime}(y,t-x) + f^{(k)\prime}(y,t+x)\right],$$

$$q(x,y) = -4\frac{d}{dx}w^{(0)}(x,y,x-0).$$

Later we find c(x) and the density $\rho(x,y) = \frac{\sigma(x,y)}{c(x)}$.

N- approximation of M.G. Krein equation in matrix-vector form

$$2\Phi(x,t) - \sum_{|m|\le N} \int_{-x}^{x} F(t-s)\Phi(x,s)ds = G, \qquad t \in (-x,x), k_j = -\overline{N,N}, j = 1,2.$$

Here $\Phi(x,t) = \left(\Phi^{(-N)}(x,t), \dots, \Phi^{(0)}(x,t), \dots, \Phi^{(N)}(x,t)\right)^T$,

$G = \left(G^{(-N)}, \dots, G^{(0)}, \dots, G^{(N)}\right)^T$ and $G^{(k)} = -\int_{-\pi}^{\pi} \frac{e^{i(k,y)}}{\rho(0,y)} dy.$

$$F(t) = \begin{vmatrix} f_{-N}^{(-N)'} & f_{-N+1}^{(-N)'} & \cdots & f_{0}^{(-N)'} & \cdots & f_{N}^{(-N)'} \\ f_{-N}^{(-N+1)'} & f_{-N+1}^{(-N+1)'} & \cdots & f_{0}^{(-N+1)'} & \cdots & f_{N}^{(-N+1)'} \\ \vdots & \vdots & \cdots & \vdots & \cdots & \vdots \\ f_{-N}^{(0)'} & f_{-N+1}^{(0)'} & \cdots & f_{0}^{(0)'} & \cdots & f_{N}^{(0)'} \\ \vdots & \vdots & \cdots & \vdots & \cdots & \vdots \\ f_{-N}^{(N)'} & f_{-N+1}^{(N)'} & \cdots & f_{0}^{(N)'} & \cdots & f_{N}^{(N)'} \end{vmatrix}$$

Discretization of M.G. Krein equation

After discretization $x_n = nh$, n is the number of partitions of the grid and replacing the integral by a finite sum, we obtain the system of linear algebraic equations:

$$(2I - hA)\Phi = G$$

$$A = \begin{vmatrix} F(0) & F(-h) & \dots & F((2n-1)h) \\ F(h) & F(0) & \dots & F((2n-2)h) \\ \vdots & \vdots & \ddots & \vdots \\ F((2n-1)h) & F((2n-2)h) & \dots & F(0) \end{vmatrix}$$

Matrix *A* has a block-Toeplitz structure. A is a square matrix of the size $2n \times (2N+1)$, where n is the number of partitions of the grid and N is the number of Fourier coefficients.

Numerical methods for solving the inverse problem

Usual approaches:

finite-difference scheme inversion,
minimizing the cost functional (solve the direct and adjoint problem on every iteration).

By solving the GLK-equation:

Monte-Carlo method (solution of the integral equation represented as Neumann series).

Discretized version of GLK-equation:

Stochastic iterative projection method (randomized version of Kaczmarz algorithm),
Utilizing the block-Toeplitz structure of the matrix.

Most fast Toeplitz solvers can be divided into two parts:
Levinson type – based on the factorization of A^{-1}
Schur type: – based on the factorization of A

We used the block-Toeplitz fast solver, proposed by V. Voevodin and E. Tyrtyshnikov, that based on the Levinson (Levinson-Durbin) recursion method.

Toeplitz matrix inversion

Traditional methods: $O(n^3)$ operations (Gauss-Jordan eliminations)

Using the Toeplitz structure:

- ***Fast*** methods: $O(n^2)$ operations (Levinson, Durbin, Trench, Zohar, Chandrasekaran, Sayed, Gohberg, Kailath, Olshevsky, Gu ...)
- ***Superfast*** methods: $O(n \log^p n)$ operations, $O(n)$ memory requirements (Martinsson, Tygert, Rokhlin, Ammar, Gragg, Stewart, Codevico, van Barel, Heinig, Chandrasekaran, Gu, Xia, Zhu ...)

Superfast preconditioner: $O(n \log n)$ operations, $O(n)$ memory requirements (Chan, Chan, Strang, Yeung, Di Benedetto, Jin, Kailath, Olshevsky, Ku, Kuo, Strela, Tyrtyshnikov, ..).

Main aspects: speed, **stability.**

The dimension of matrices in applications

Let *h* be the mesh size.

After discretization of Gelfand-Levitan-Krein equation we obtain the following system

$$(2I - hA) = G,$$

$$A = \begin{pmatrix} F'(0) & F'(h) & \dots & F'((2n-1)h) \\ F'(h) & F'(0) & \dots & F'((2n-2)h) \\ \vdots & \ddots & \ddots & \vdots \\ F'((2n-1)h) & F'((2n-2)h) & \dots & F'(0) \end{pmatrix}$$

Therefore the matrix A has the dimension $2n \times (2N+1)$

where n is the mesh size, N is the number of Fourier coefficients.

In 2D in the domain **3 x 3 km^2** with **h=5m** and number of Fourier coefficients is equal to 50 matrix has a dimension **120.000^2**.

For the cube **3 x 3 x 3 km^3** – matrix has the dimension **12.000.000^2**.

Fast inversion of block-Toeplitz matrix

Algorithm developed by V.V. Voevodin and E.E. Tyrtyshnikov and is based on a consistent solution of truncated (embedded) systems. The algorithm is based on the recursive Levinson-Durbin method.

Let us consider the sequence of the problems (k=0,..N)

$$A_k = \begin{pmatrix} a_0 & a_{-1} & \dots & a_{-k} \\ a_1 & a_0 & \dots & a_{-k+1} \\ \vdots & \ddots & \ddots & \vdots \\ a_k & a_{k-1} & \dots & a_0 \end{pmatrix}$$ - leading submatrix.

$$A_k z_k = b_k = \begin{pmatrix} b_0 \\ b_1 \\ \vdots \\ b_k \end{pmatrix}$$

Embedded systems correspond to the Gelfand-Levitan-Kerin equations for a shallower depth.

We are looking for the solution of auxiliary systems (the first and last columns of the inverse matrix):

$$A_k x_k = e_k^{(1)} = \begin{pmatrix} 1 \\ 0 \\ \vdots \\ 0 \end{pmatrix}, A_k y_k = e_k^{(k+1)} = \begin{pmatrix} 0 \\ \vdots \\ 0 \\ 1 \end{pmatrix}$$

Inverse problem solution at point x requires O($N^2 n^2$) operations (usual approach - O($N^3 n^3$)).
Inverse problem solution on (0,x) requires O($N^2 n^2$) operations (usual approach - O($N^3 n^4$)).

V.V. Voevodin, E.E. Tyrtyshnikov. Computational processes with Toeplix matrices. Moscow, 1987.

S.I. Kabanikhin, N.S. Novikov, I.V. Oseledets, M.A. Shishlenin. Fast Toeplitz linear system inversion for solving 2D acoustic inverse problem. J. Inverse and Ill-Posed Problems, 2015. 23(6).

Reconstruction

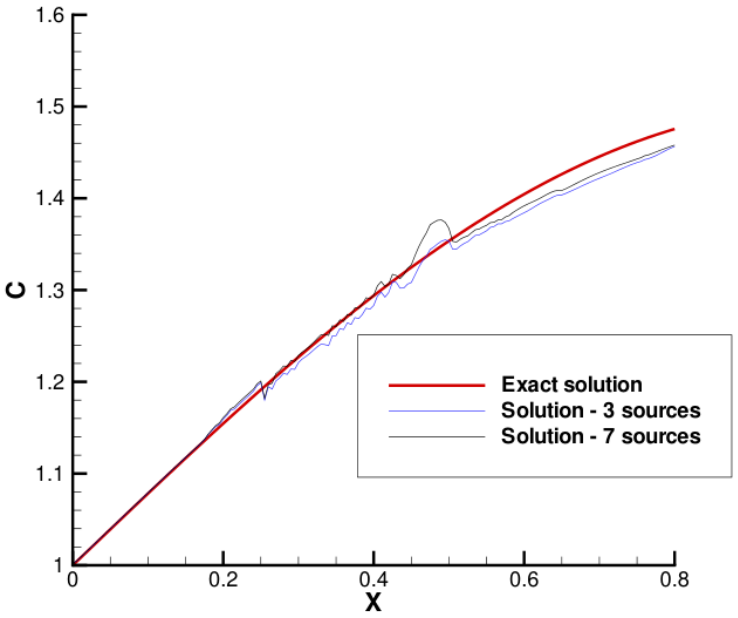

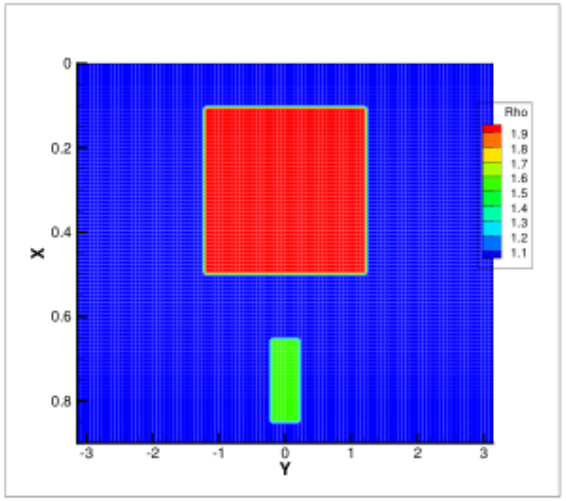

(a)

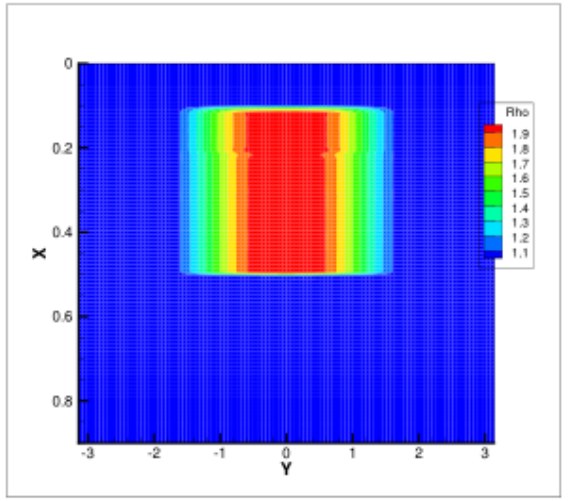

(b)

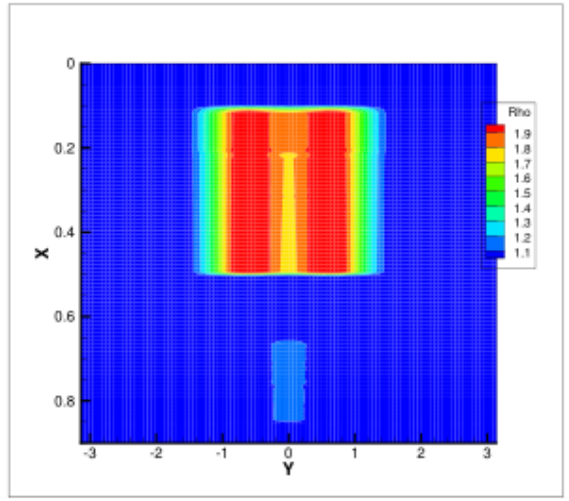

(c)

(a) – точное решение, (b) – 5 источников/приемников, (c) – 9 источников/приемников

Numerical stability. Conditional number of the matrix

Exact data

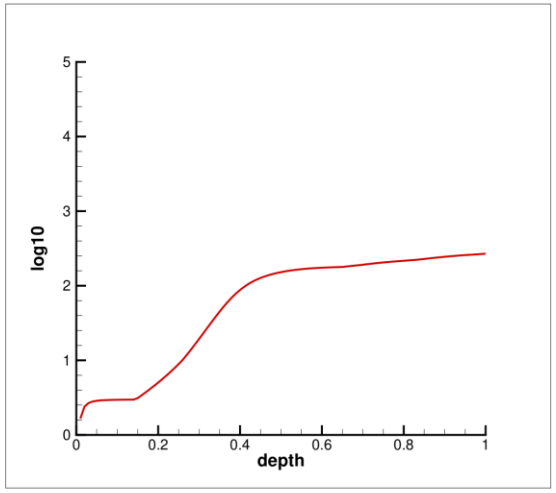

$T = 1,\ N_x = 100,\ N = 10$

Exact data

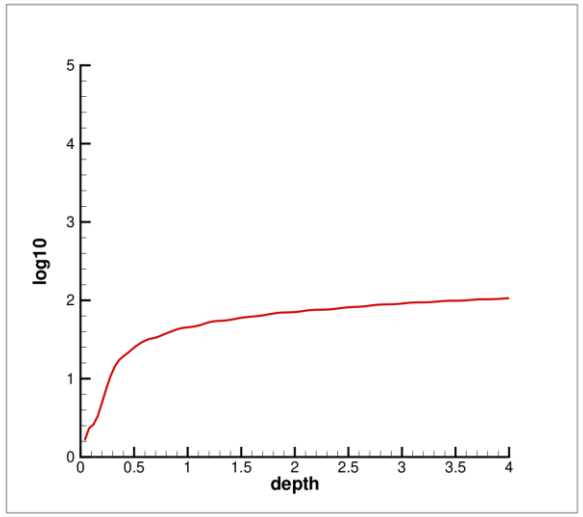

$T = 4,\ N_x = 100,\ N = 10$

Noisy data

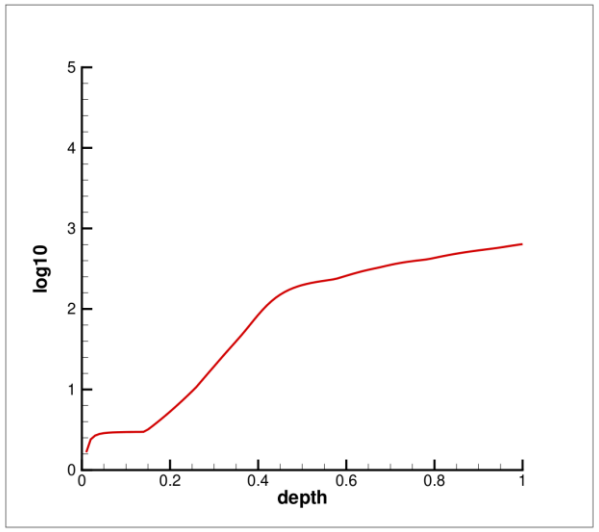

$T = 1,\ N_x = 100,\ N = 10$

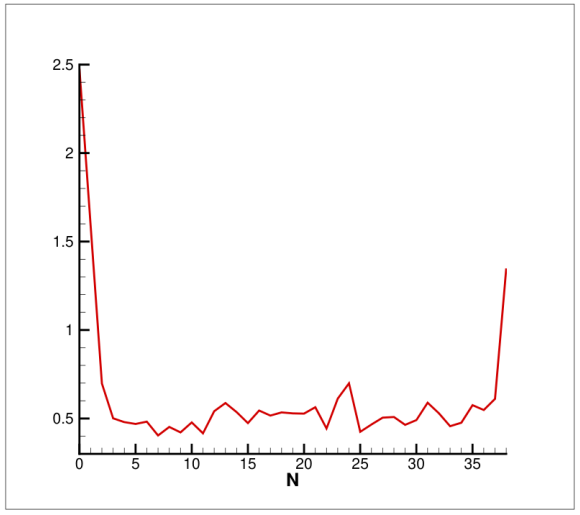

Discrepancy.
The number of sources and receivers are regularization number.

It is possible to determine the optimal number of sources and receivers for a particular noise in the inverse problem data.

Inverse problem. Optimization

Direct problem

$$\frac{\partial u}{\partial t}+\frac{1}{\rho}\frac{\partial p}{\partial x}=0$$

$$\frac{\partial v}{\partial t}+\frac{1}{\rho}\frac{\partial p}{\partial y}=0$$

$$\frac{\partial p}{\partial t}+\sigma p+\rho c^2\left(\frac{\partial u}{\partial x}+\frac{\partial v}{\partial y}\right)=\Theta_\Omega(x,y)I(t)$$

$$\Omega=(\mathrm{x},\mathrm{y})\in[0{:}\,L]\times[0{:}\,L]$$

$$(\mathrm{x},\mathrm{y})\in\Omega$$
$$0<t<T$$

Initial data $u,v,p\Big|_{t=0}=0$

Non-reflective boundary conditions

Inverse problem: find ρ, c, σ in Ω

$p(x_i,y_i,t)=f_i(t)$ - *pressure measured in detectors*

Ricker wavelet

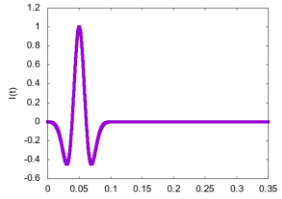

$$I(t)=\left(1-2\left(\pi\nu_0\left(t-\frac{1}{\nu_0}\right)\right)^2\right)e^{-\pi\nu_0\left(t-\frac{1}{\nu_0}\right)}$$

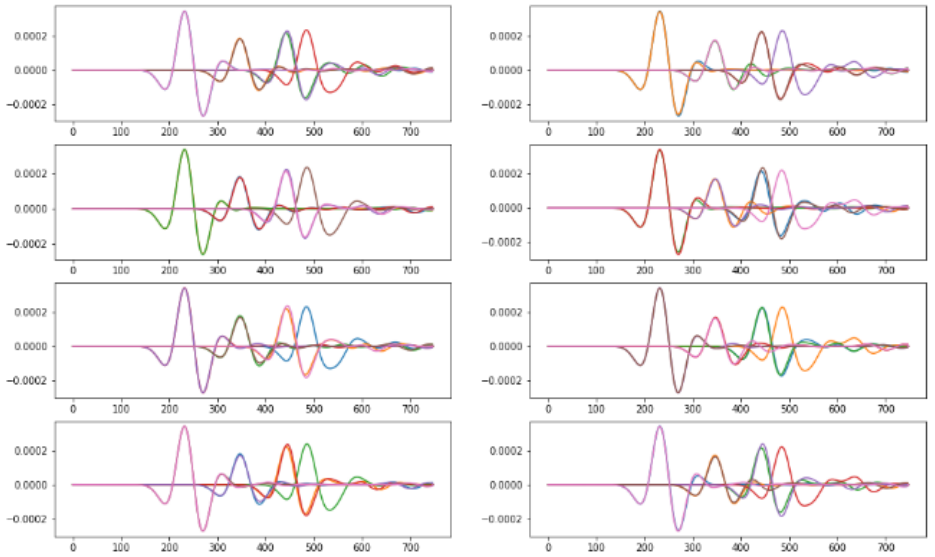

T.D. Mast, L.M. Hinkelman, L.A. Metlay, M.J. Orr, R.C. Waag. Simulation of ultrasonic pulse propagation, distortion, and attenuation in the human chest wall. J. Acoust. Soc. Am. (1999) 106, 6.

V.G. Romanov, S.I. Kabanikhin. Inverse problems of geoelectrics, 1991.

A.L. Bukhgeĭm, Extension of solutions of elliptic equations from discrete sets, J. Inverse Ill-Posed Problems. 1993. 1(1).

V.G. Romanov, D.I. Glushkova. The problem of determining two coefficients of a hyperbolic equation. Dokl. Math. 2003. 67:3.

O. Imanuvilov, V. Isakov, M. Yamamoto. An inverse problem for the dynamical Lame system with two sets of boundary data. Comm. Pure Appl. Math. 2003, 56.

L. Beilina, M. Cristofol, S. Li, M. Yamamoto. Lipschitz stability for an inverse hyperbolic problem of determining two coefficients by a finite number of observations. Inverse Probl. 2017, 34, 015001.

M.V. Klibanov, J. Li, W. Zhang. Convexification for the inversion of a time. dependent wave front in a heterogeneous medium. SIAM J. Appl. Math. 2019. 79(5).

M.V. Klibanov, A. Timonov. Acoustic Imaging via a Viscosity Approximation of an Elliptic System Generated by the Lavrentiev Integral Operator. SIAM J. Imagine Sciences. 2025. 18(2).

M.V. Klibanov, J. Li, V.G. Romanov, Z. Yang. Carleman Numerical Method for Imaging of Moving Targets. https://arxiv.org/abs/2512.18361v1.

Optimization

$$A(q) = f, \qquad J(q) = \|A(q) - f\|^2 \to \min_{q=(c,\rho,\sigma)}$$

$$J(q) = \int_0^T \sum_{i=1}^{N} [p(x_i, y_i, t; q) - f_i(t)]^2 dt \to \min_{q=(c,\rho,\sigma)}$$

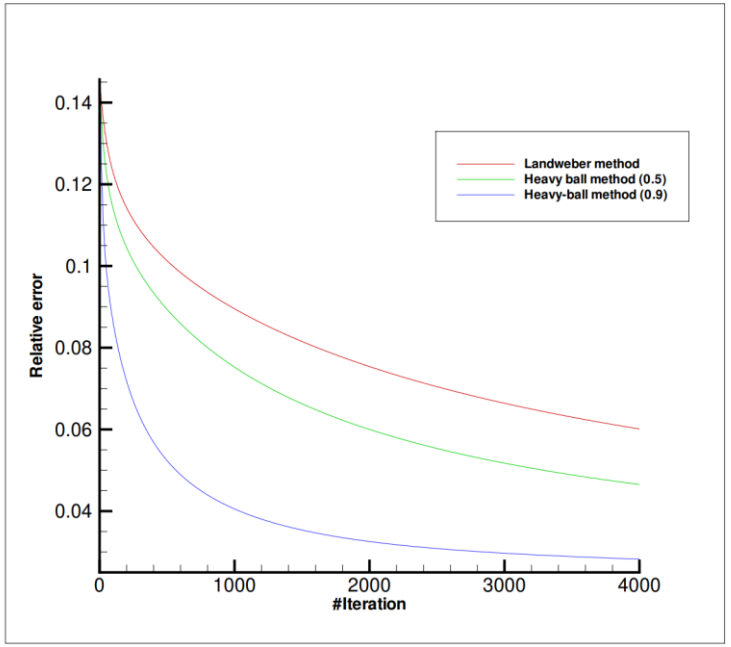

Landweber iteration: $q_{n+1} = q_n - \alpha_n [A'(q_n)]^* (A(q_n) - f)$

$$J'(q_n) = 2[A'(q_n)]^* (A(q_n) - f)$$

Heavy-ball method: $q_{n+1} = q_n - \alpha_n J'(q_n) + \beta_n (q_n - q_{n-1})$

Nesterov method: $q_{n+1} = q_n - \alpha_n J'(q_n + \beta_n (q_n - q_{n-1})) + \beta_n (q_n - q_{n-1})$

M. Hanke. Accelerated Landweber iterations for the solution of ill-posed equations. Numer. Math. 1991. 60.

A. Neubauer. On Nesterov acceleration for Landweber iteration of linear ill-posed problems. J. Inverse and Ill-posed Problems. 2017. 25(3).

S. Kindermann. Optimal-order convergence of Nesterov acceleration for linear ill-posed problems. Inverse Problems. 2021. 37, 065002.

d'Aspremont, D. Scieur, A. Taylor. Acceleration Methods. Foundations and Trends® in Optimization. 2021. 5(1–2).

Kabanikhin S.I., Klychinskiy D.V., Kulikov I.M., Novikov N.S., Shishlenin M.A. Direct and inverse problems for conservation laws. Continuum Mechanics, Applied Mathematics and Scientific Computing: Godunov's Legacy: A Liber Amicorum to Professor Godunov, 2020.

N.S. Novikov, M.A. Shishlenin, D.V. Kluchinskiy. Comparative Analysis of Two Gradient-Based Approaches to Inverse Problem of Ultrasound Tomography. Days on Diffraction, 2024.

Gradient

$$\boldsymbol{\rho_{n+1} = \rho_n - \alpha_\rho J'(\rho_n), c_{n+1} = c_n - \alpha_c J'(c_n), \sigma_{n+1} = \sigma_n - \alpha_\sigma J'(\sigma_n)}$$

$$\mathrm{J}'(\rho) = \int_0^T \left[-u\psi_{1_t} - v\psi_{2_t} + \frac{\psi_3}{\rho}\left(u_x + v_y\right) \right] dt$$

$$\mathrm{J}'(c) = \int_0^T \frac{\psi_3}{c^2}\left(u_x + v_y\right) dt$$

$$\mathrm{J}'(\sigma) = \int_0^T \frac{p(x,y,t)\Psi_3(x,y,t)}{\rho c^2(x,y)} dt.$$

u, v, p - direct problem solution

ψ_1, ψ_2, ψ_3 - adjoint problem solution

$$\frac{\partial \psi_1}{\partial t} + \frac{1}{\rho}\frac{\partial \psi_3}{\partial x} = 0 \qquad \frac{\partial \psi_2}{\partial t} + \frac{1}{\rho}\frac{\partial \psi_3}{\partial y} = 0$$

$$\frac{\partial \psi_3}{\partial t} - \sigma\psi_3 + \rho c^2\left(\frac{\partial \psi_1}{\partial x} + \frac{\partial \psi_2}{\partial y}\right) = 2\sum_{i=1}^{N} \delta(x - x_i, y - y_i)[p - f_i]$$

$$\psi_1, \psi_2, \psi_3 \Big|_{t=T} = 0$$

Non-reflective boundary conditions

S. He, S. Kabanikhin. An optimization approach to a 3D acoustic inverse problem in the time domain. J. Mathematical Physics. 1995. 36 (8).

M. Gustafsson, S. He. An optimization approach to multi-dimensional TD acoustic inverse problems. J. Acoustical Society of America. 2000. 108, 1548.

Kabanikhin S.I., Klyuchinskiy D.V., Novikov N.S., Shishlenin M.A. Numerics of acoustical 2D tomography based on the conservation laws. J. Inverse and Ill-Posed Problems, 2020, 8(2).

Klyuchinskiy D., Novikov N., Shishlenin M.A. Modification of gradient descent method for solving coefficient inverse problem for acoustics equations. Computation. 2020, 8(3), № 73.

Gradient methods: $q_{n+1} = q_n - \alpha\left(A'(q_n)\right)^*(A(q_n) - f)$

[Hanke, Neubauer, Scherzer, 1995]: the gradient method converges locally if the conditions are met in some neighborhood of the exact solution:

1. $\|A'(q)\| \le \mu < 1$,
2. $\|A(x) - A(y) - A'(y)(x - y)\| \le \eta\|A(x) - A(y)\|$, $0 < \eta < 1/2$.

Holds $\|q_{n+1} - q_{exact}\| \le M\beta^{n+1}$, $0 < \beta < 1$.

M.Hanke, A.Neubauer, O.Scherzer. A convergence analysis of the Landweber iteration for nonlinear ill-posed problems. Numer. Math. 1995. 72.
S. Kabanikhin. Regularization of the Volterra operator equation of the first kind with a limited Lipschitz-continuous kernel. DAN USSR. 1989. 39(3).
S. Kabanikhin, O. Scherzer, M. Shishlenin. Iteration methods for solving a two-dimensional inverse problem for a hyperbolic equation. J. Inverse and Ill-Posed Problems. 2003. 11(1).

Using a priori information about the solution: smoothness, monotony… At each iteration, the approximate solution is projected into the desired class of functions.

24

Vasin V.V., Eremin I.I. Operators and iterative processes of the Feyerian type. Theory and applications. 2005.
Kabanikhin S.I., Shishlenin M.A. Quasi-solution in inverse coefficient problems. J. Inverse and Ill-Posed Problems. 2008, 16(6).

Theoretical Results

$$\frac{dy}{dt} = F(y(t), y, \boldsymbol{p}), t \in (0, T) \qquad y(0) = \boldsymbol{y_0} \qquad y(t) = \left(y_1(t), y_2(t), \dots, y_N(t)\right)$$

Some parameters of the model p and y_0 are unknown. We have additional information

$$y_i(t) = \boldsymbol{f_i(t)}$$

The direct (and inverse) problem is reduced to a system of Volterra integral equations.

$$\boldsymbol{y(t) = y_0 + \int_0^t F_\tau(y) d\tau}$$

Theorem (on local well-posedness). Exists $T^* \in (0, T)$, such that for all $t \in (0, T^*)$, the solution exists in L_2, unique and continuously depends on the data.

Theorem (on correctness in the vicinity of the exact solution). Let for some $\boldsymbol{y_0}$ the solution exists $y \in L_2$. Then there is such δ, that for any $\boldsymbol{y_o^\delta}$: $\left|\left|\boldsymbol{y_0 - y_o^\delta}\right|\right| < \boldsymbol{\delta}$ solution exist, unique and решение уравнения continuously depends on the data.

S. Kabanikhin. Regularization of the Volterra operator equation of the first kind with a limited Lipschitz-continuous kernel. DAN USSR. 1989. 39(3).
S.I. Kabanikhin, O. Scherzer, M.A. Shishlenin. Iteration methods for solving a two-dimensional inverse problem for a hyperbolic equation. J. Inverse and Ill-Posed Problems. 2003. 11(1).

Recovering density when the velocity is unknown

True density

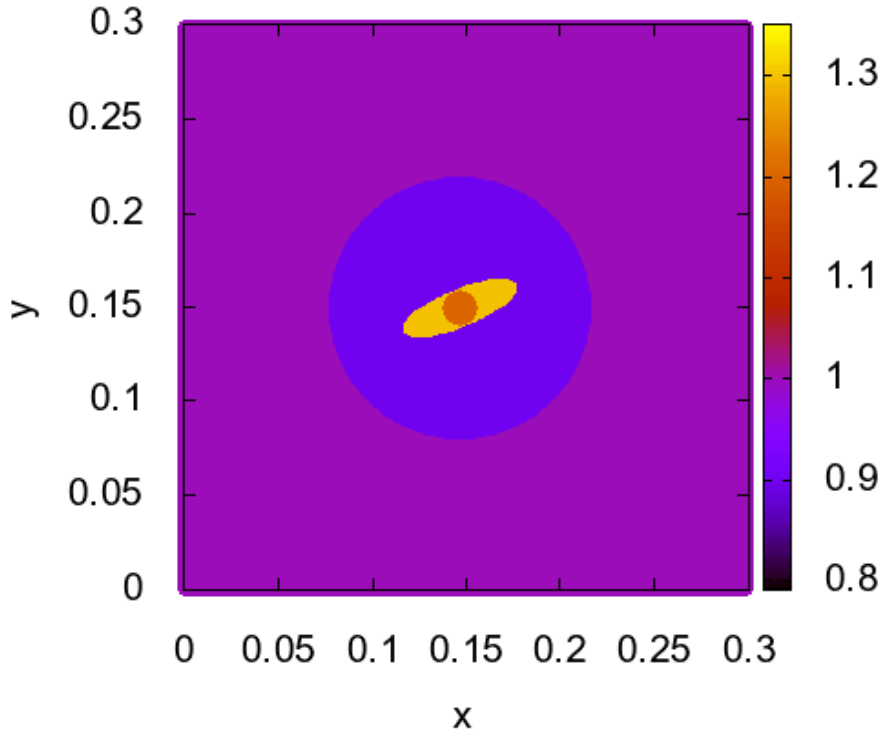

True velocity

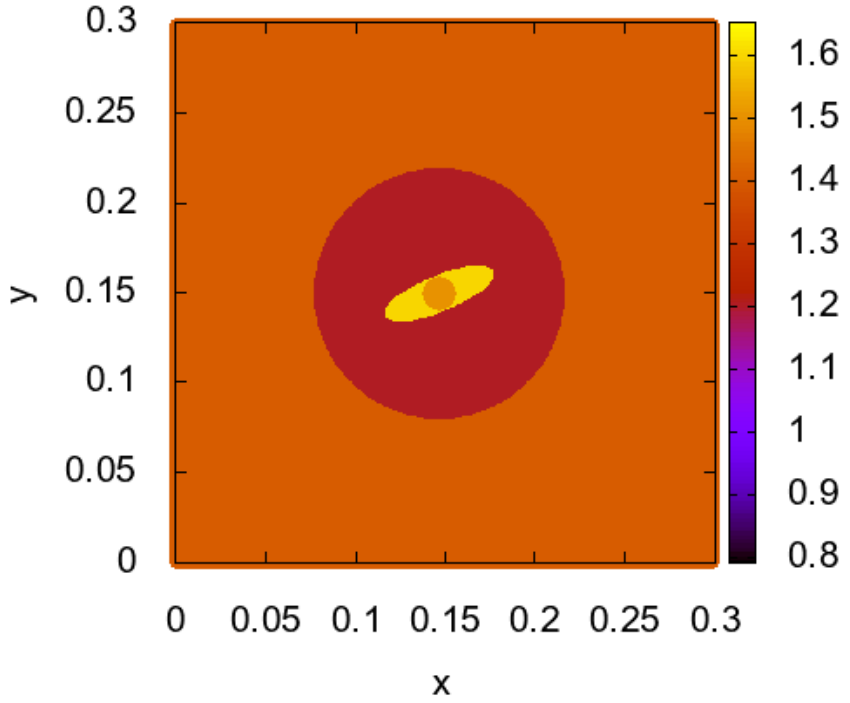

The filler – water, the domain considered – fat inside the inclusions with higher density.

Initial guess does not contain information about inclusions.

How the uncertainty in the velocity depends on the density?

True velocity

Inverse problem solution (1000 iterations, mesh size is 3 mm, 8 sources and receivers)

Velocity is known exactly

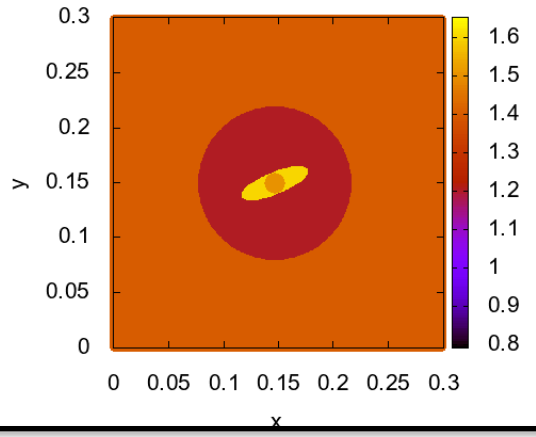

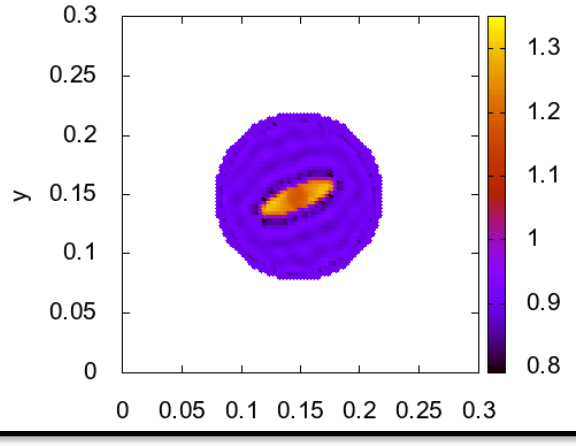

Velocity is known approximately

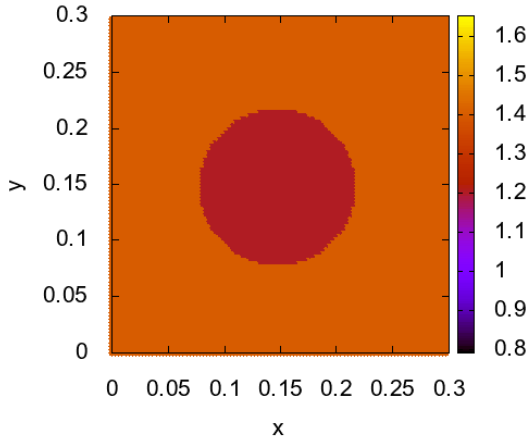

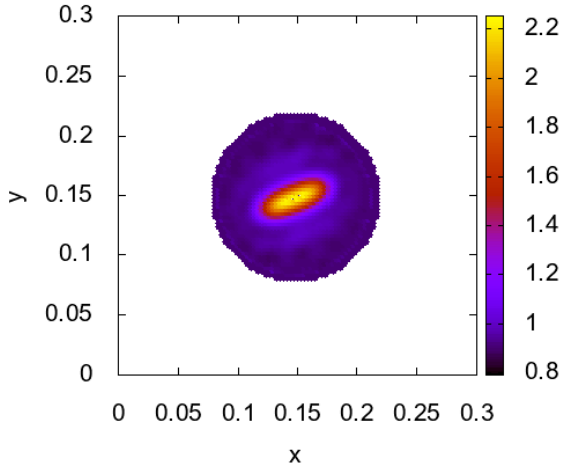

Optimization of RAM memory and CPU time

$$J'(\rho) = \int_0^T \left[-u\psi_{1_t} - v\psi_{2_t} + \frac{\psi_3}{\rho}(u_x + v_y) \right] dt$$

The usual approach

1) Solve the direct problem $p_j(x_i, y_i, t; q_n)$
2) Solve the adjoint problem
3) Calculate the gradient $J_j' = J_j'(q_n)$

Simultaneous scheme

1) Solve the direct problem $p_j(x_i, y_i, t; q_n)$
2) Solve the adjoint problem and find the solution on particular time and calculate the gradient $J_j' = J_j'(q_n)(t_n)$

Standard scheme

Mesh size	CPU Time, s			Memory, Gb
	4 cores	8 cores	16 cores	
$N_x = N_y = 100$	2.9	1.5	1.1	0.18
$N_x = N_y = 200$	23.8	11.8	7.2	1.43
$N_x = N_y = 400$	184.1	96.2	53.7	11.48

Simultaneous scheme

Mesh size	CPU Time, s			Memory, Gb
	4 cores	8 cores	16 cores	
$N_x = N_y = 100$	2.29	1.26	0.83	0.09
$N_x = N_y = 200$	18.1	9.37	5.56	0.72
$N_x = N_y = 400$	145.3	75.12	42.03	5.75

The calculation of the conjugate problem and the gradient is optimized in terms of the consumed RAM resources and calculation time. The optimized version of the algorithm provides better results both in terms of RAM requirements (50% improvement) and in terms of computing time (10-25 % depending on the number of cores).

D. Klyuchinskiy, N. Novikov, M. Shishlenin. CPU-time and RAM memory optimization for solving dynamic inverse problems using gradient-based approach. J. Computational Physics. 2021. 439, 110374.

3D inverse problem

The grid is 120 x 120 x 120.
500 iterations.
The **3d IP** calculation time on Intel Xeon Gold 6140 (2.1 Ghz, 18 cores) is **70 hours**.
2d IP – 7 hours.

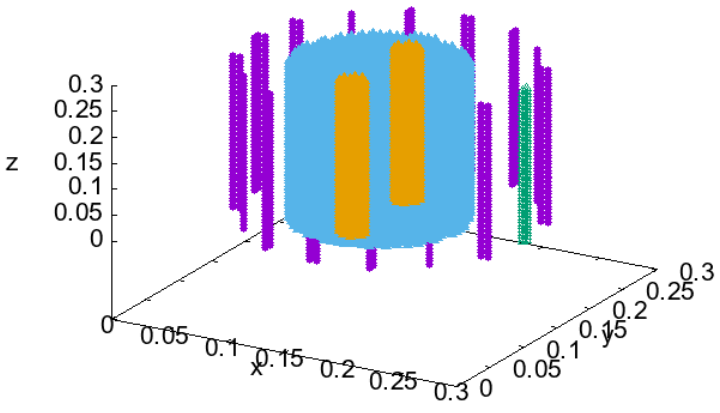

True

Numerical inverse problem solution

Density

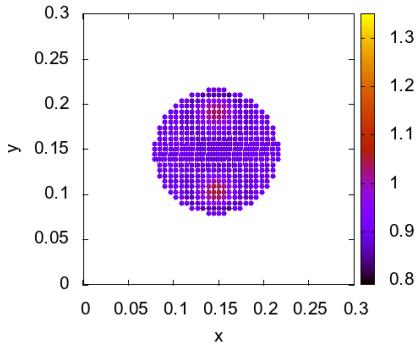

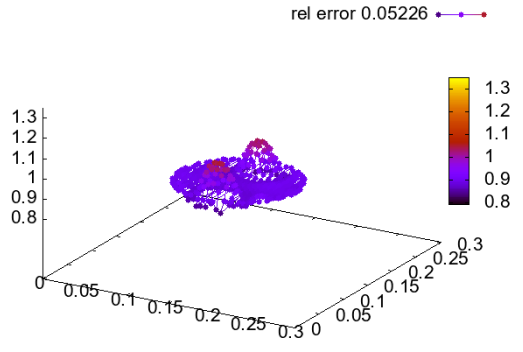

Velocity

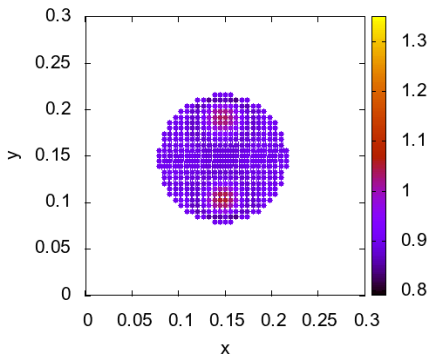

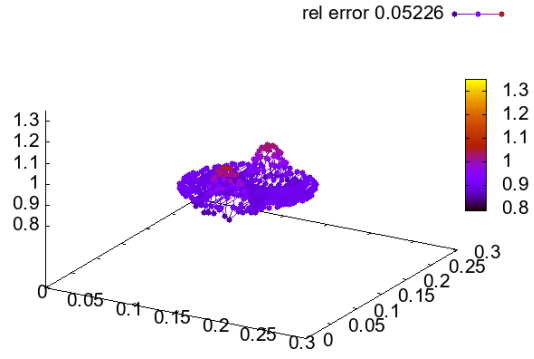

D. Klyuchinskii, N. Novikov, M. Shishlenin. On the numerical reconstruction of the 3D density of the medium in the acoustic system of equations. Siberian Electronic Mathematical Reports. 2024. 21(2).

Newton-Kantorovich type methods

Direct problem:

$$\frac{\partial u}{\partial t}+\frac{1}{\rho}\frac{\partial p}{\partial x}=0 \qquad \frac{\partial v}{\partial t}+\frac{1}{\rho}\frac{\partial p}{\partial y}=0 \qquad \frac{\partial p}{\partial t}+\rho c^2\left(\frac{\partial u}{\partial x}+\frac{\partial v}{\partial y}\right)=\Theta_\Omega(x,y)I(t)$$

Newton-Kantorovich:

$$\boldsymbol{q_{n+1}=q_n-\left(A'(q_n)\right)^{-1}(A(q_n)-f)}$$

$$\frac{\partial \psi_1}{\partial t}+\frac{1}{\rho}\frac{\partial \psi_3}{\partial x}=\frac{\breve{\rho}(x,y)}{\rho}\frac{\partial u}{\partial t}$$

$$\frac{\partial \psi_2}{\partial t}+\frac{1}{\rho}\frac{\partial \psi_3}{\partial y}=\frac{\breve{\rho}(x,y)}{\rho}\frac{\partial v}{\partial t}$$

$$\frac{\partial \psi_3}{\partial t}-\sigma\psi_3+\rho c^2\left(\frac{\partial \psi_1}{\partial x}+\frac{\partial \psi_2}{\partial y}\right)=-\breve{\rho}(x,y)c^2\left(\frac{\partial u}{\partial x}+\frac{\partial v}{\partial y}\right)$$

Inverse problem data:

$$\psi_3(x,y,t)=p(x_i,y_i,t)-f(x_i,y_i,t)$$

Convergence – 10-20 iterations

The initial approximation is close to the exact solution

Instability.

Gradient method:

$$\boldsymbol{q_{n+1}=q_n-\alpha_n[A'(q_n)]^*(A(q_n)-f)}$$

$$\frac{\partial \psi_1}{\partial t}+\frac{1}{\rho}\frac{\partial \psi_3}{\partial x}=0 \qquad \frac{\partial \psi_2}{\partial t}+\frac{1}{\rho}\frac{\partial \psi_3}{\partial y}=0$$

$$\frac{\partial \psi_3}{\partial t}-\sigma\psi_3+\rho c^2\left(\frac{\partial \psi_1}{\partial x}+\frac{\partial \psi_2}{\partial y}\right)=$$

$$2\sum_{i=1}^{N}\Theta_{\Omega_i}[p(x_i,y_i,t)-\boldsymbol{f_i}(t)]$$

Convergence at least 1000 iterations

One solver for direct (linear) and adjoin problem.

Kinematic inverse problem

8 sensors, the sensors are located at a distance of 15 cm from the center: 56 arrival times of the waves.

Speed of sound: water - 1435 m/s, brain - 1510-1540 m/s.

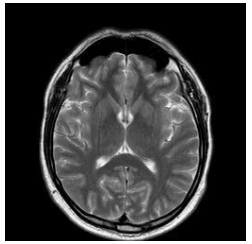

$$\|\nabla\tau\|^2 = c^{-2}(x, y, z)$$

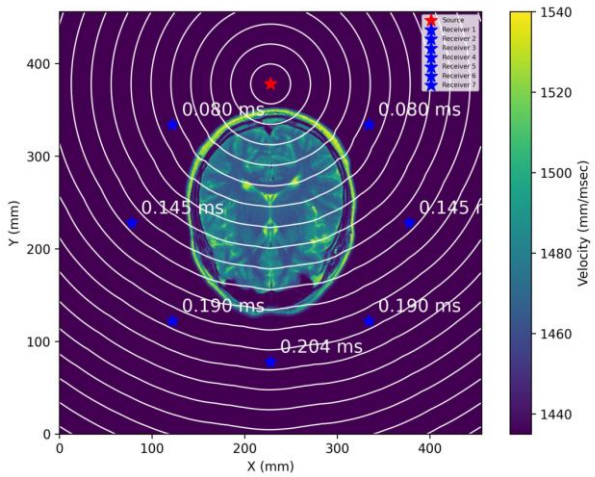

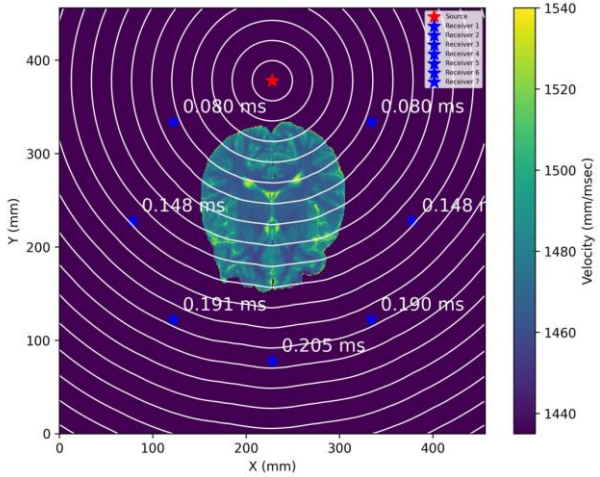

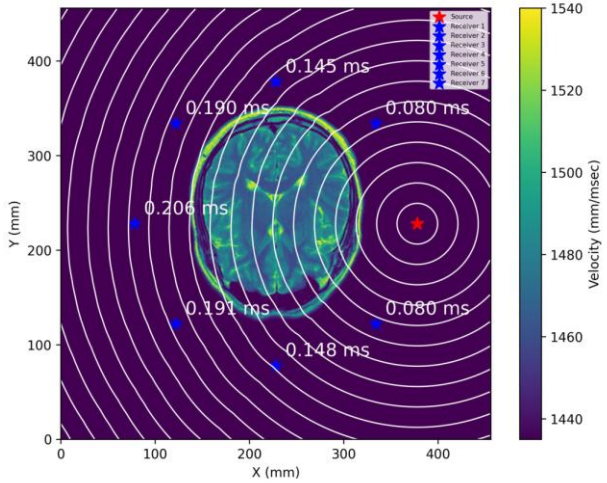

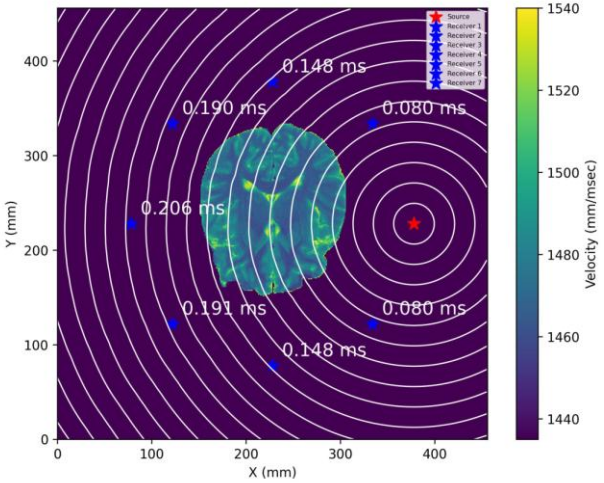

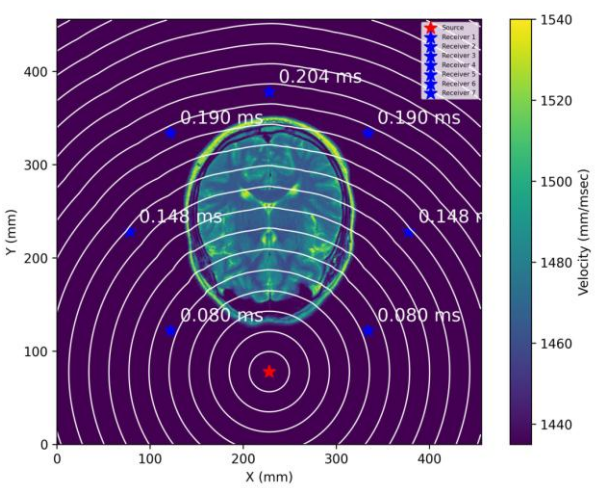

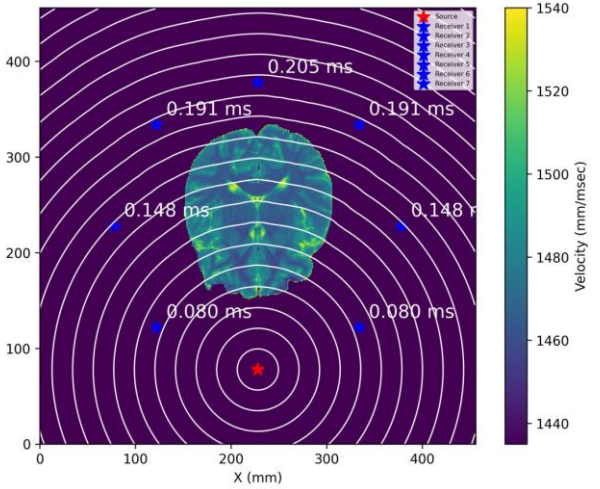

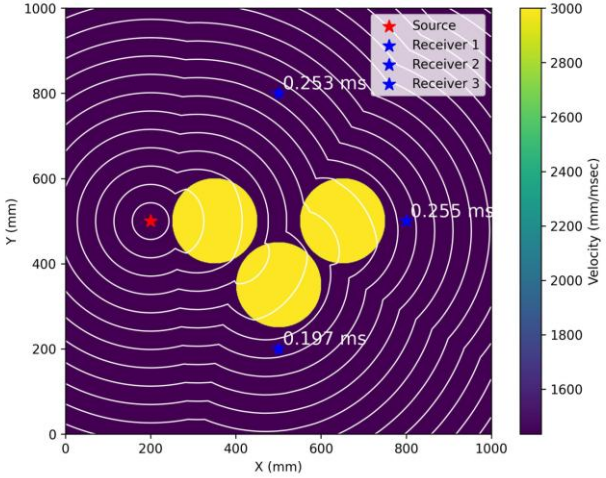

8 receivers: 56 wave arrival times.

256 receivers: 65280 times.

Combined kinematic and dynamic inverse problem

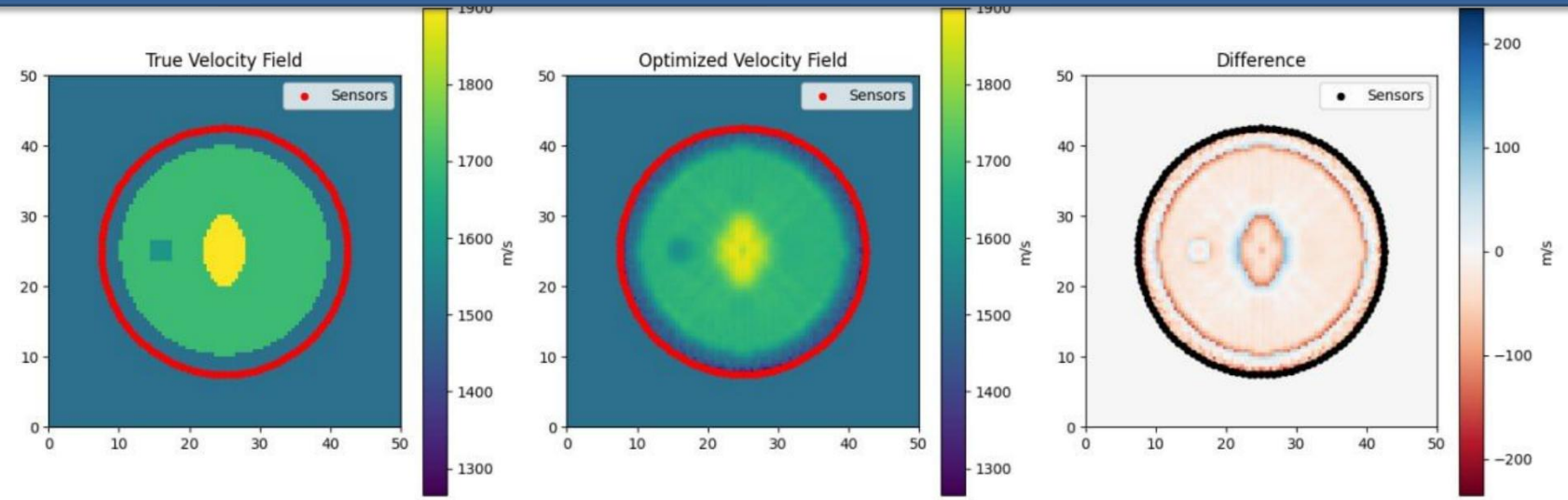

128 sources and receivers

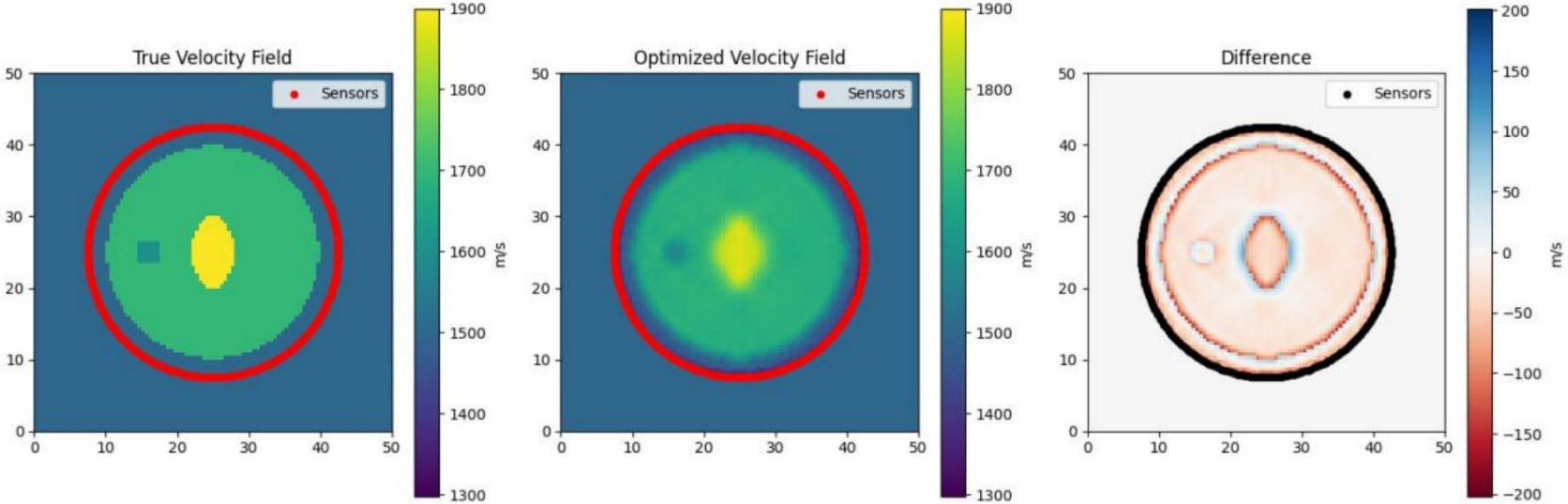

256 sources and receivers

Kabanikhin S., Shishlenin M., Novikov N., Dudar M. Combined inverse problems of 2d medical ultrasound tomography: dynamic and kinematic approach. J. Inverse and Ill-Posed Problems. 2026, 34(2).

Deep learning in acoustic tomography

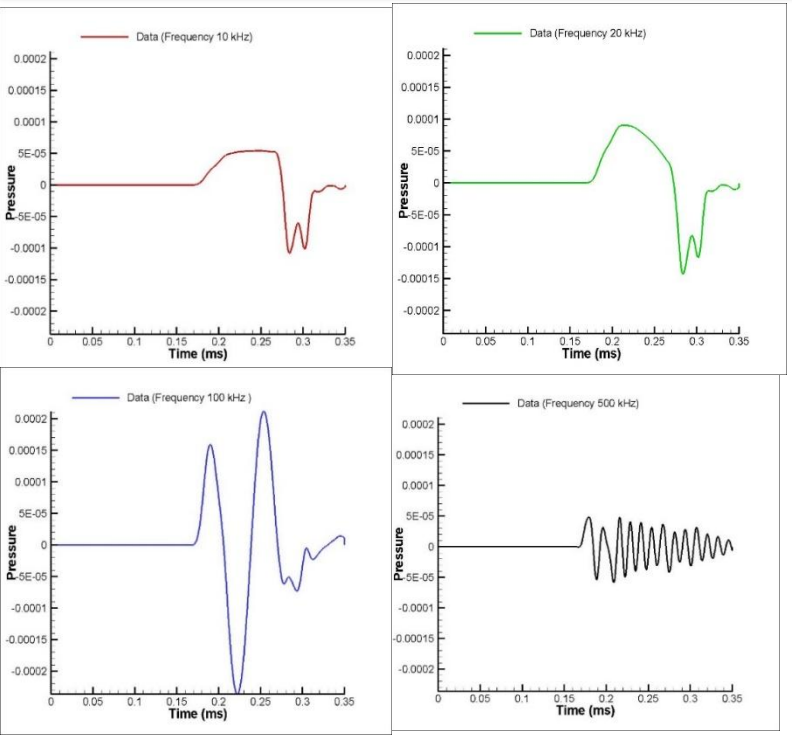

Acoustic pressure data measured in receivers

Acoustic pressure data

?

Neural networks

Mathematical model

Coefficient inverse problem

?

Restoration of acoustic parameters of the environment

2D

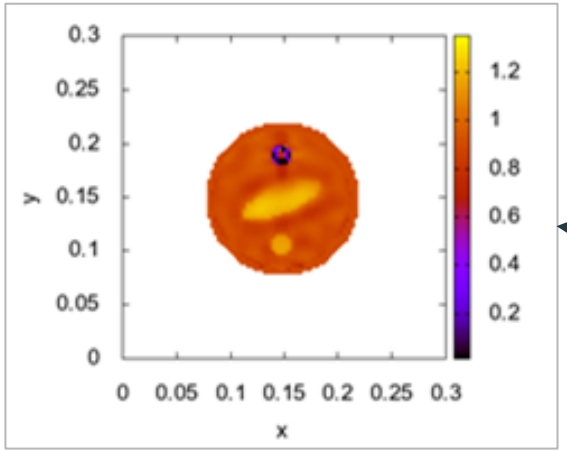

To recover the speed of sound propagation in the medium c(x, y), the density of the medium $\rho(x,y)$ and acoustic attenuation

Autoencoder NN. Modernization

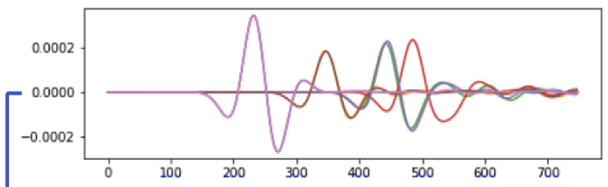

Curve #1

Curve #56

Conv block

Conv block

Conv block

Conv block

Concat

Conv block

Dim=256

Latent space

Conv block

Reshape 4x4

8x8

Up block

6x16

Up block

2x32

Up block

4x64

Up block

28x1

Up block

Conv 1x1

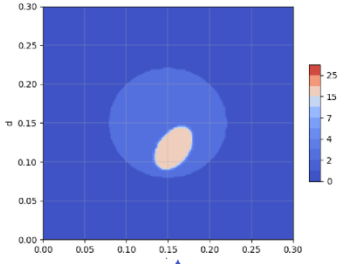

Conv block = 1 dimConv + BatchNorm + Activation

Up block = ConvTranspose + BatchNorm + Activation

NN numerical solution

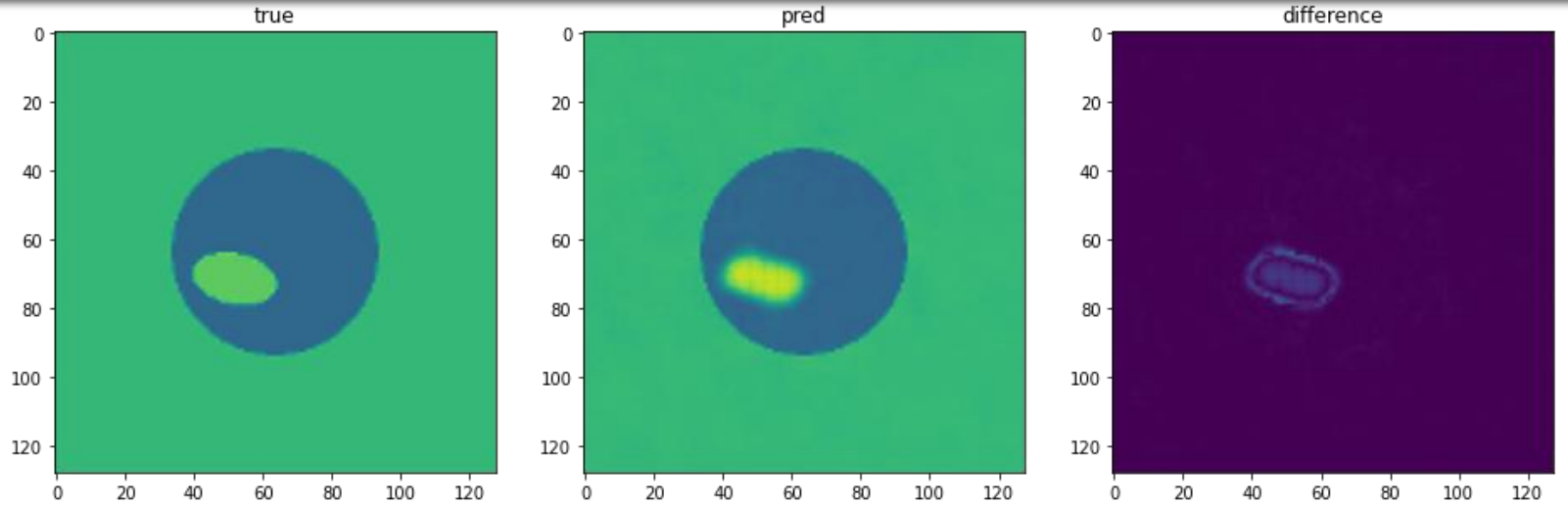

True solution(left), computed solution(center), difference (right). MSE = 0.021

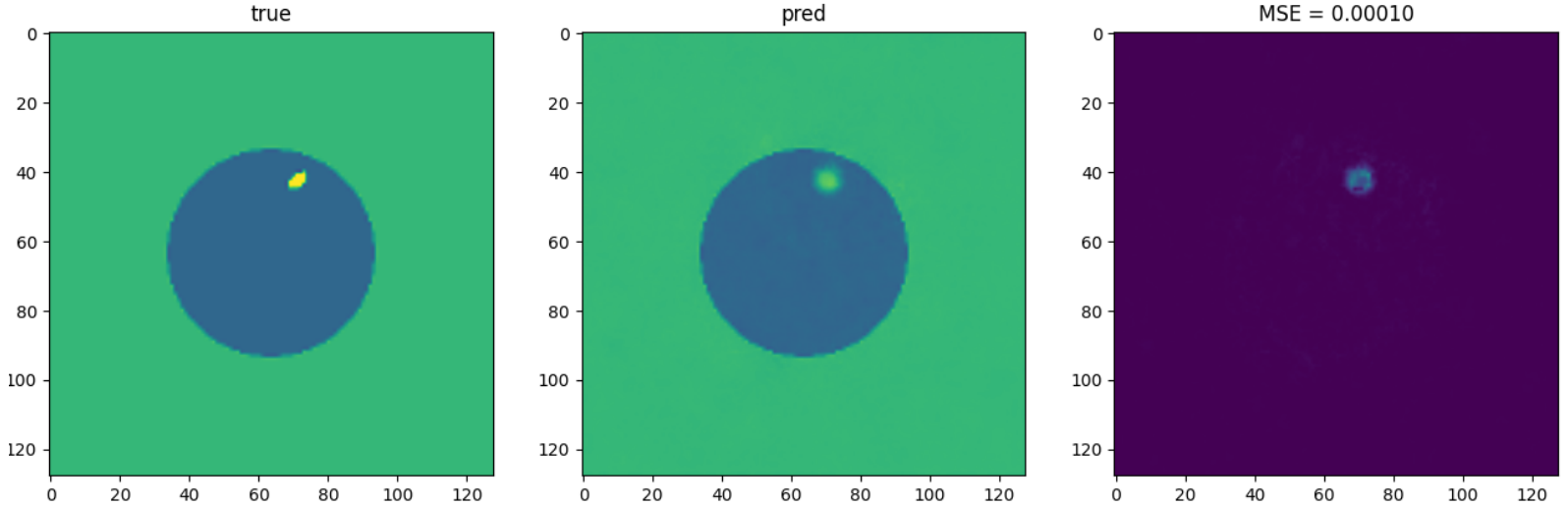

True solution(left), computed solution(center), difference (right). MSE = 0.011

A. Prikhodko, M. Shishlenin, N. Novikov, D. Klyuchinskiy. Encoder neural network in 2D acoustic tomography. Applied and Computational Mathematics. 2024. 23(1).

NN numerical solution

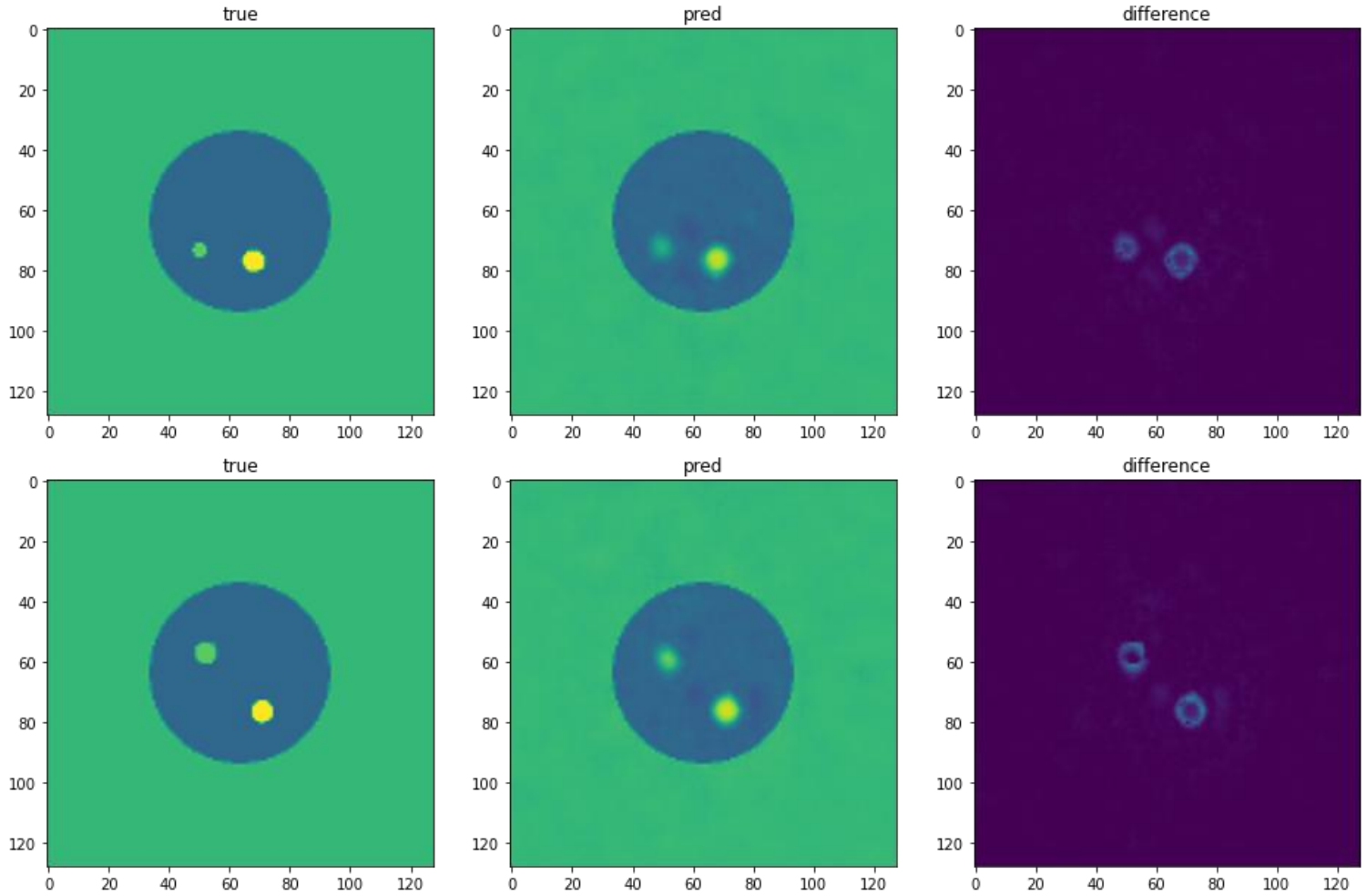

Application of AI in inverse and ill-posed problems:

S. Arridge, P. Maass, O. Oktem, C. Schonlieb. Solving inverse problems using data-driven models. Acta Numerica. 2019. 28.

J. Berg, K. Nystrom. Neural networks as smooth priors for inverse problems for PDEs, J. Computational Mathematics and Data Science. 2021. 1, 100008.

Comparative analysis:

- Intel Xeon Gold 6140 (2.1 Ghz, 18 threads), RAM 512 Gb - 7 hours for coefficient inverse problem solution.
- Intel i5-10400F (2.9 GHz, 6 threads), GeForce RTX 2070, RAM 64 Gb - 0,01 sec. for inverse problem solution based on Deep learning. Before it we need 35 hours for learning.

NN numerical solution

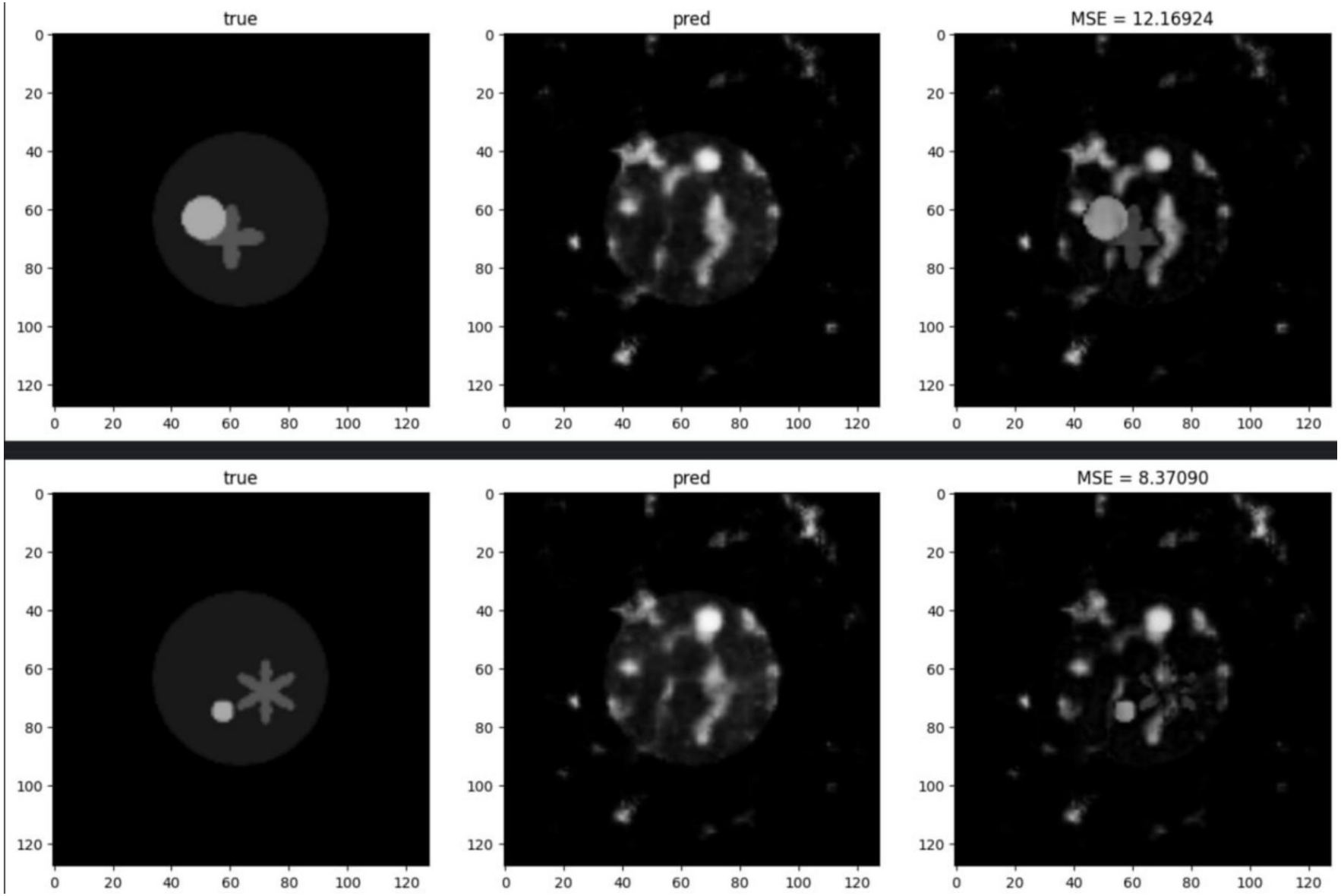

Conditional stability of NN

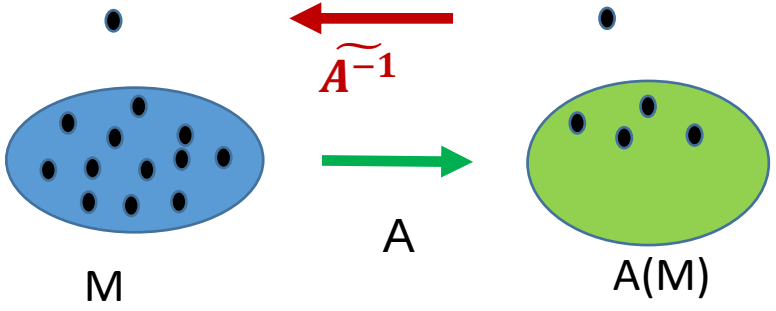

Operator form of inverse problem:

$$\boldsymbol{A(q) = f, q = A^{-1}(f)}$$

Here q is solution, f is a data.

Neural networks is approximation $\widetilde{A^{-1}}$ of inverse operator A^{-1} on datasets (M).

M.M. Lavrentiev proposed to identify a class of conditionally stability problems. Let Q, F are topological spaces and $M \subset Q$ is fixed set. Let $A(M)$ be a image of the set M when map $A: Q \to F$, so $A(M) = \{f \in F: \exists q \in M \; such \; that \; A(q) = f\}$.

Definition (conditional well-posedness, Tikhonov well-posedness).

Problem $A(q) = f$ is called conditional well-posed on the set M, if $f \in A(M)$ and the following conditions:

1) Solution q_E of $A(q) = f, f \in A(M)$, is unique on M;

2) for any neighborhood $O(q_T)$ the solution of the equation $A(q) = f$ there is a neighborhood $O(f)$ such that for any $f_\delta \in O(f) \cap A(M)$ the solution of $A(q) = f_\delta$ is contained in $O(q_T)$ (*conditional stability*).

In the second condition, only such variations f_δ of data f, are allowed that do not derive from the existence class of $A(M)$.

M is called the well-posedness set of the problem $A(q) = f$.

V.V. Vasin, I.A. Gainova. On methods of conditional convex minimization generating regularizing algorithms. Proceedings of the Institute of Mathematics and Mechanics. 2025. 31(4).

The stability to perturbations of an acceptable set of solutions for convex functionals on convex sets was proved!

NN numerical solution. Apriori gradient information

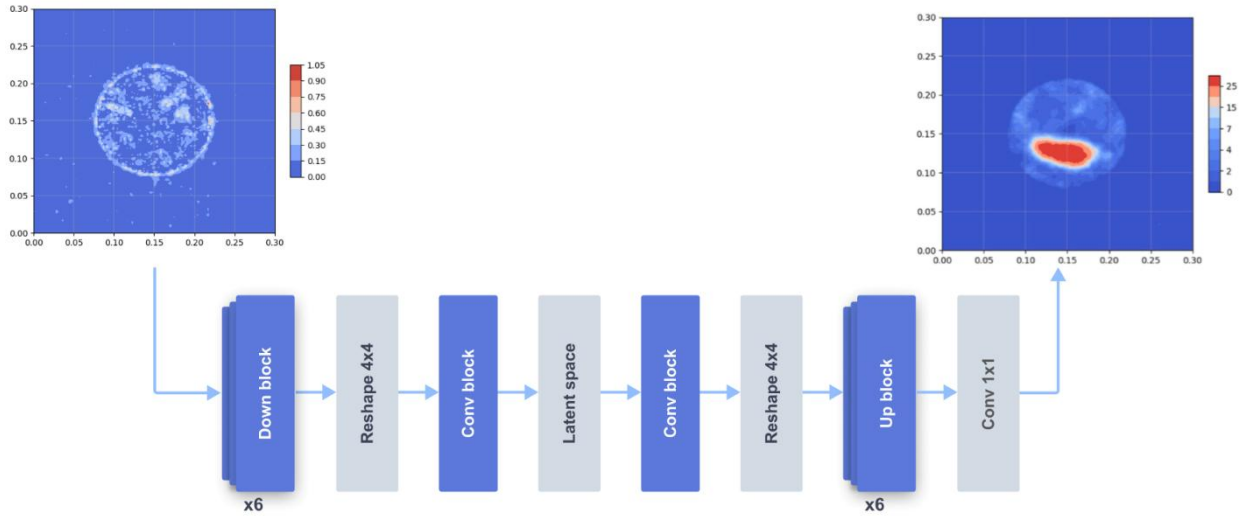

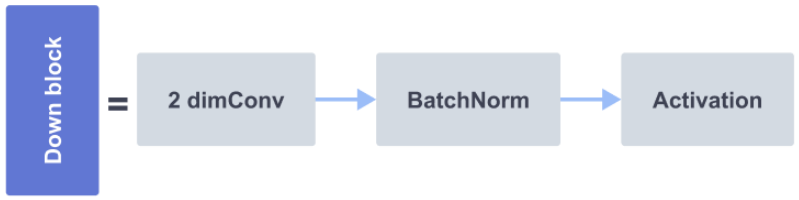

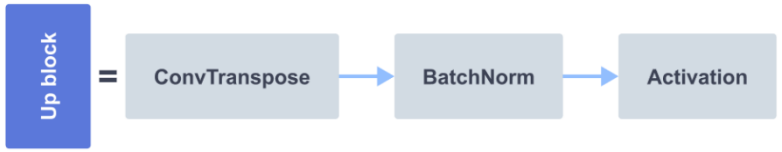

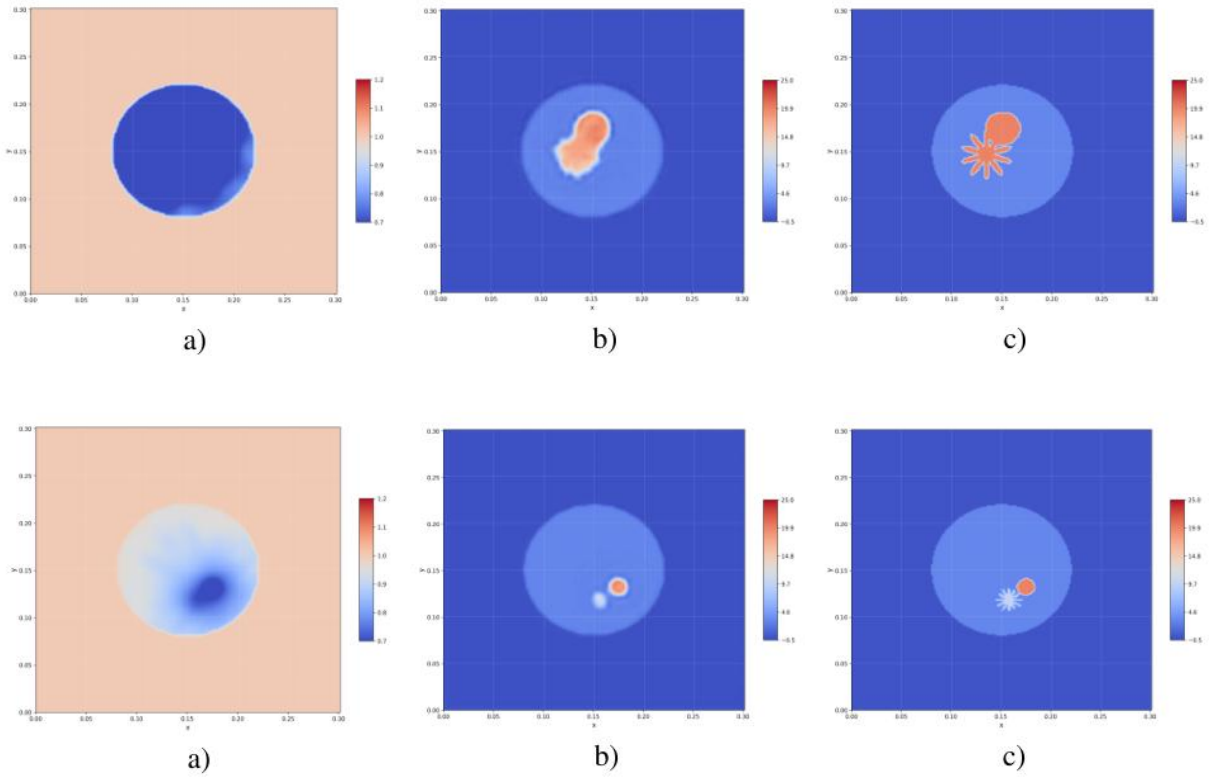

a) input b) NN solution c) exact

N. Savchenko, N. Novikov, M. Shishlenin. Convolutional Neural Networks of Recovering Acoustic Absorption in Ultrasound Tomography from Gradient Data. J. Mathematical Sciences. 2025. 292(7).

Nonlinear 3d tomography

T.G. Muir, E.L. Carstensen. Prediction of nonlinear acoustic effects at biomedical frequencies and intensities. Ultrasound in Medicine & Biology. 1980. 6(4).

G. Uhlmann – Conference Talks.

B. Kaltenbacher. Mathematics of nonlinear acoustics. Evolution Equations and Control Theory. 2015. 4(4).

F.A. Duck. Nonlinear acoustics in diagnostic ultrasound. Ultrasound in Medicine & Biology. 2002. 28(1).

T. Yu, W. Cai. Simultaneous reconstruction of temperature and velocity fields using nonlinear acoustic tomography. Appl. Phys. Lett. 2019. 115 (10).

Using the numerical solution of the Navier-Stokes equation system, it is possible to simulate the propagation of sound waves in a liquid.

DNS is currently not used due to the computational cost.

The aim is to show the possibility of constructing a digital twin of the tomograph within the framework of a "unified" physical and mathematical model based on the Navier-Stokes equations.

The size of the modeling area is quite small, sound waves are waves of "small" disturbance, and given that a person is more than sure that 60% consists of water, then human organs can be "modeled" by a "liquid" model with their density.

Nonlinear 3d tomography

M. Shishlenin, A. Kozelkov, N. Novikov. Nonlinear Medical Ultrasound Tomography: 3D Modeling of Sound Wave Propagation in Human Tissues. Mathematics. 2024, 12, 212.

B. Kaltenbacher, P. Lehner. A first order in time wave equation modeling nonlinear acoustics. Journal of Mathematical Analysis and Applications. 2025. 543 (2), 128933

Here small amplitude approximation of a Navier-Stokes-Fourier system modeling nonlinear acoustics was considered. Omitting all third and higher order terms with respect to certain small parameters, it was obtained a first order in time system containing linear and quadratic pressure and velocity terms. Subsequently, the well-posedness of the derived system was shown using the classical method of Galerkin approximation in combination with a fixed point argument. It was proved the well-posedness of a linearized equation using energy estimates and then the well-posedness of the nonlinear system using a Newton-Kantorovich type argument. Based on this, the global in time well-posedness for small enough data and exponential decay was obtained.

F. Lucka, M. Pérez-Liva, B.E. Treeby, B.T. Cox. Inverse Problems. 2022. 38 025008

$$\left(\frac{1}{c_0{}^2(x)}\frac{\partial^2}{\partial t^2} - \rho_0(x)\nabla\cdot\left(\frac{1}{\rho_0(x)}\nabla\right) + L\nabla^2\right)p(x,t) = s(x,t)$$

$$L = \tau(x)\frac{\partial}{\partial t}\left(-\nabla^2\right)^{\frac{y}{2}-1} + \eta(x)\left(-\nabla^2\right)^{\frac{y+1}{2}-1}$$

$$\text{Absorption} — \tau(x) = -2\alpha_0(x)c_0(x)^{y-1}$$
$$\text{Dispersion} — \eta(x) = 2\alpha_0(x)c_0(x)^{y}\tan(\pi y/2)$$

We consider the following

- Liver patology
- Problems with lang after Covid-19

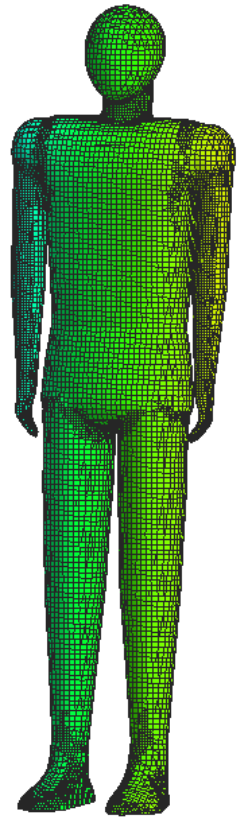

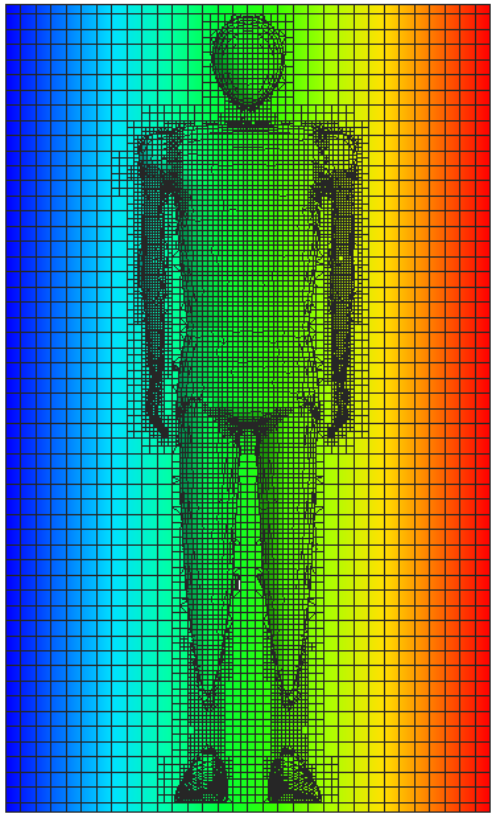

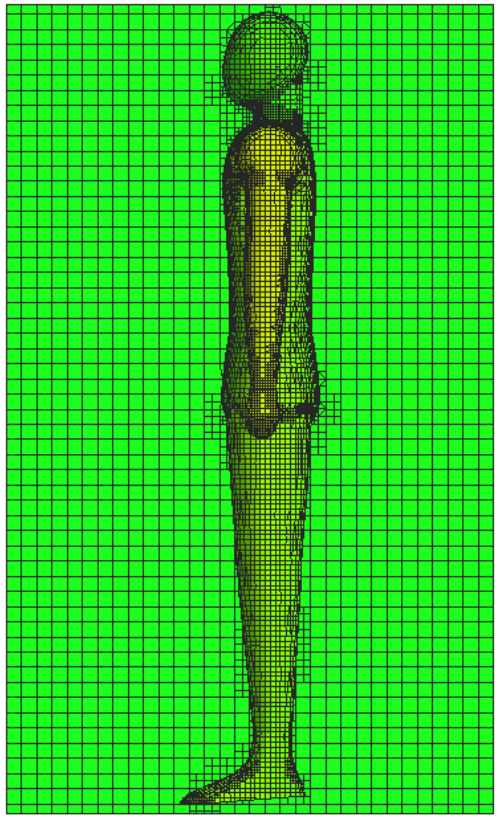

Tissue Type	Speed of Sound, m/s	Density, kg/m³
Fatty Tissue	1460	904
Muscular Tissue	1550	994
Bone Tissue	3660	1700
Liver	1570	1083
Average for Human Body	1036	1036

Parameters of 3D body:

height – 1,95 м,

shoulders – 0,56 м,

Thickness – 0,34 м.

Parameters of tomography:

Height – 2 м, diameter – 1,2 м.

Nonlinear 3D tomography

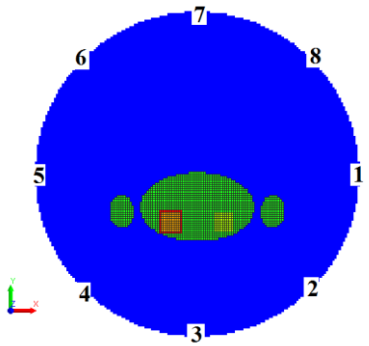

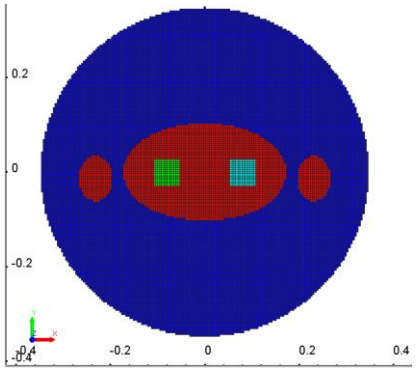

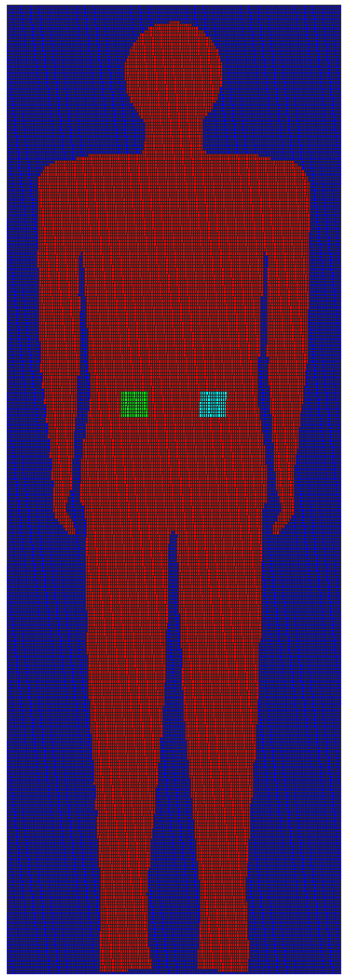

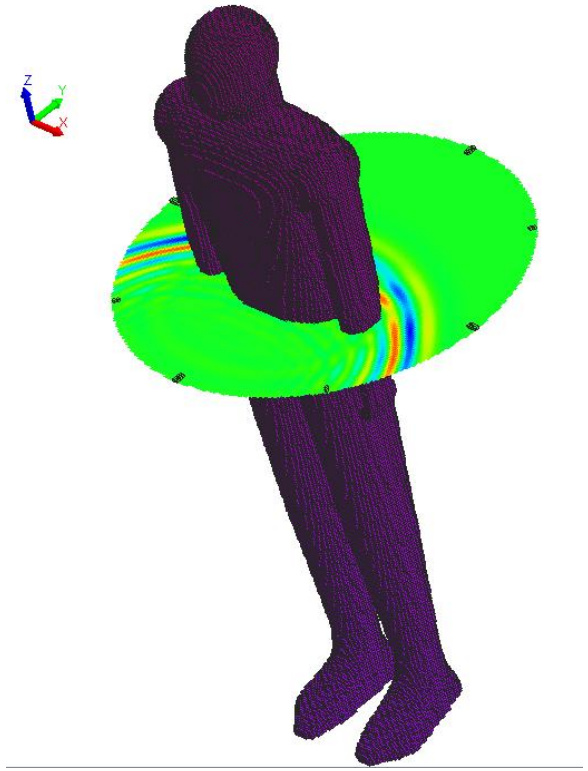

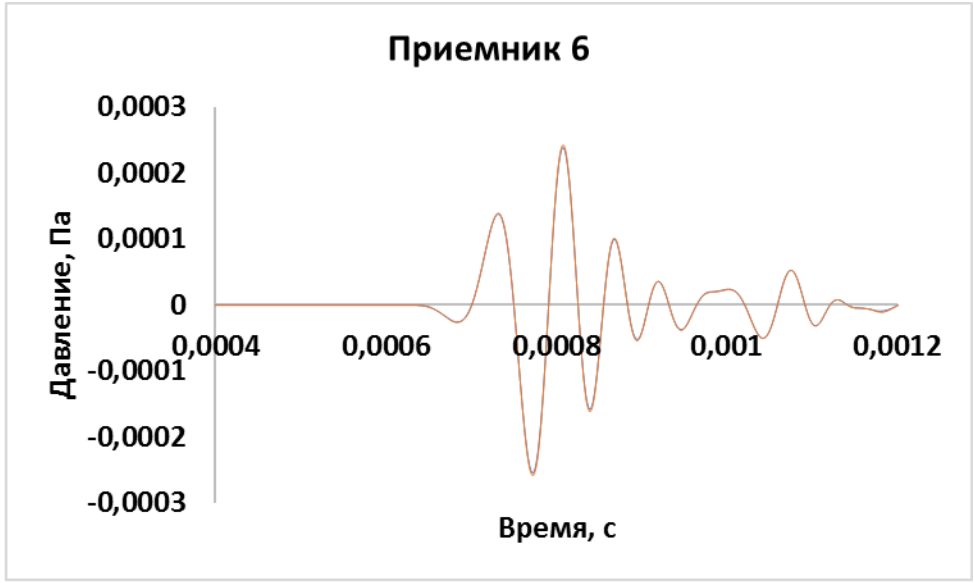

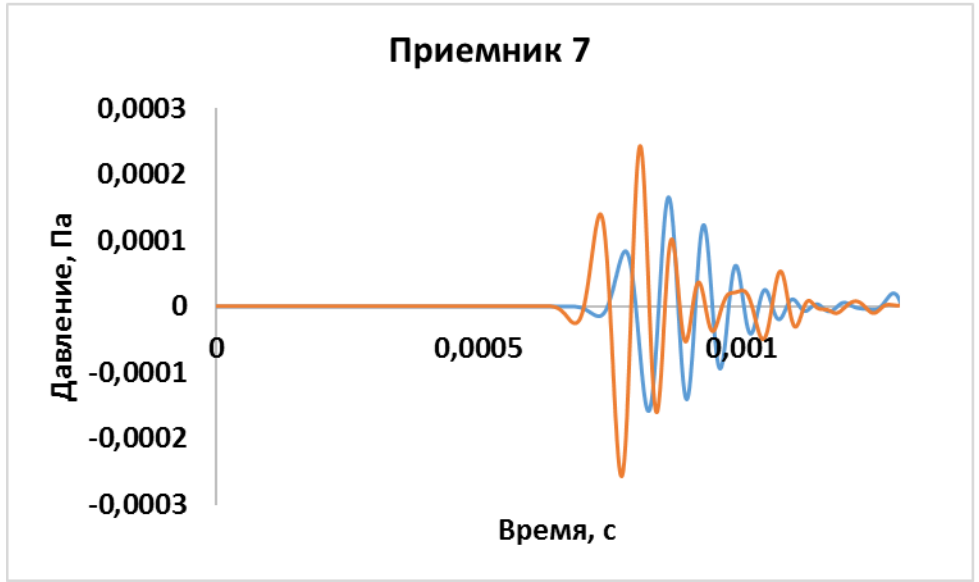

15.5 million cells, 2 days numerical calculation of Direct Problem on 20 CPU from a single source.

3d Digital Twin

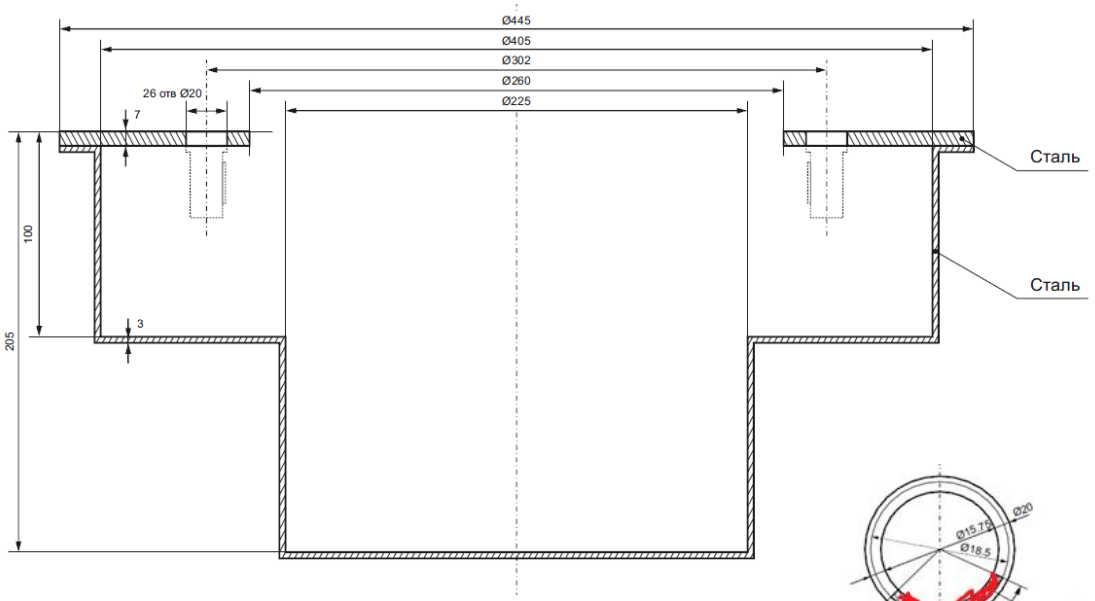

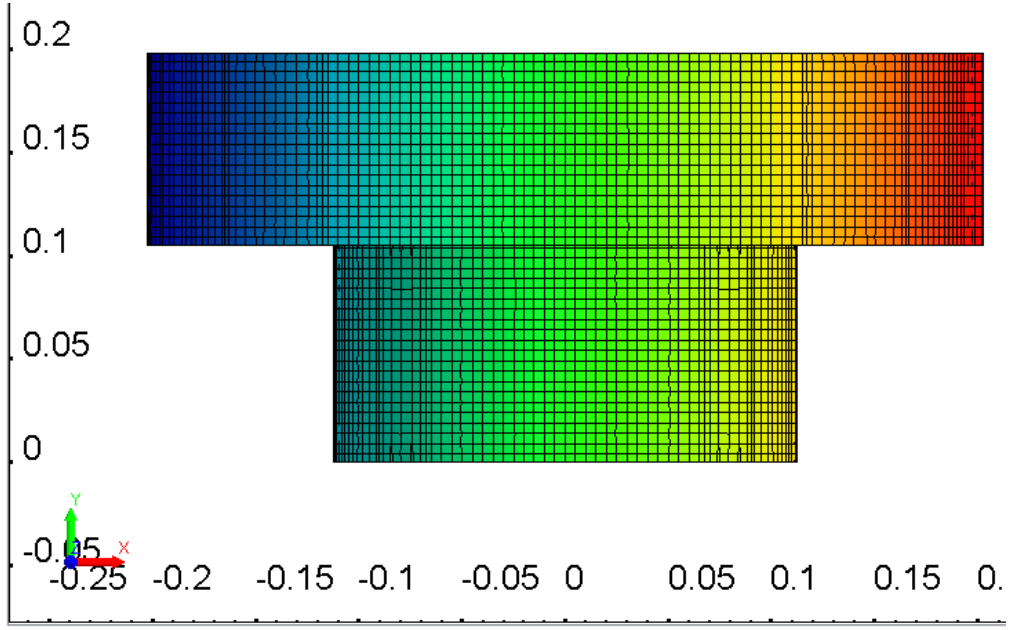

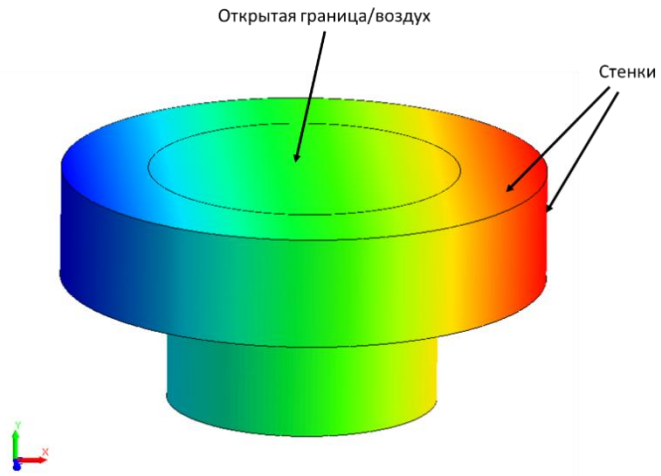

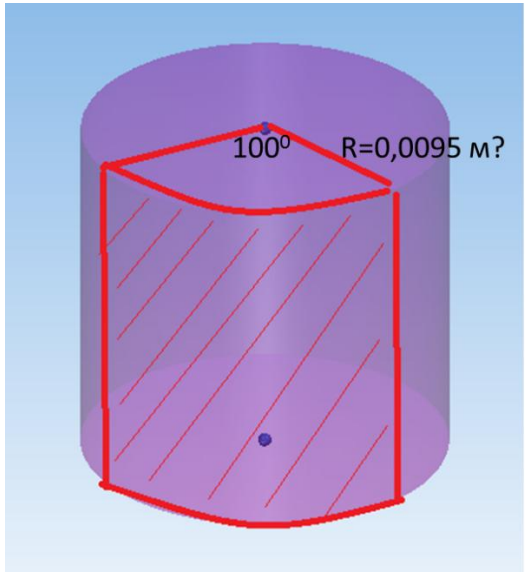

For the first time, the effect of fluid flow movement during rotation of a specific tomographic equipment on the propagation of ultrasound in water was investigated.

3d Digital Twin

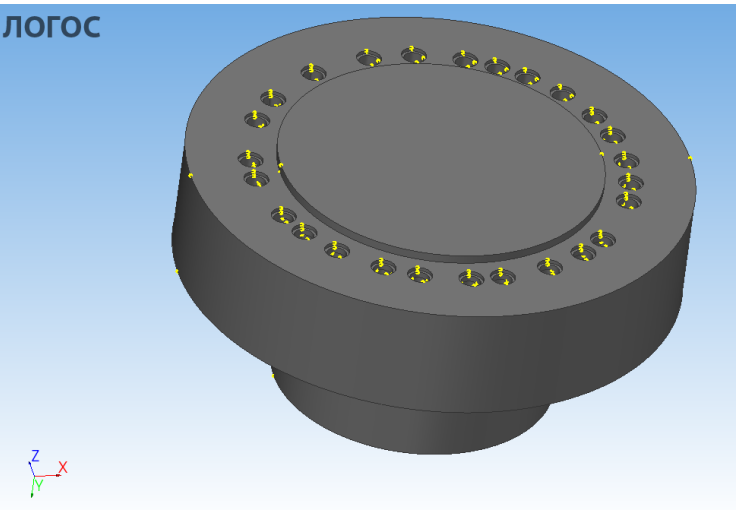

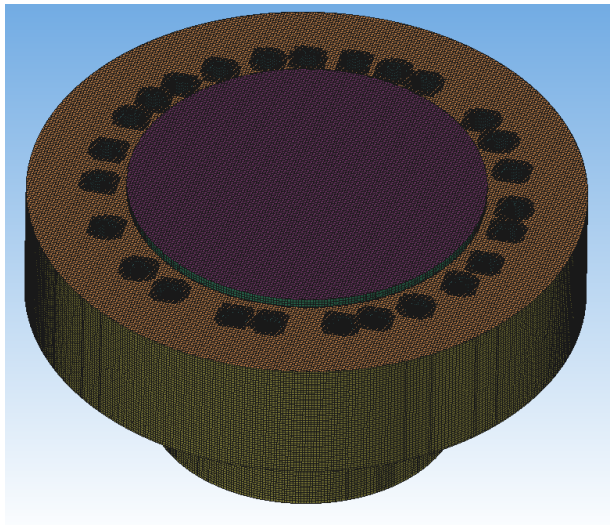

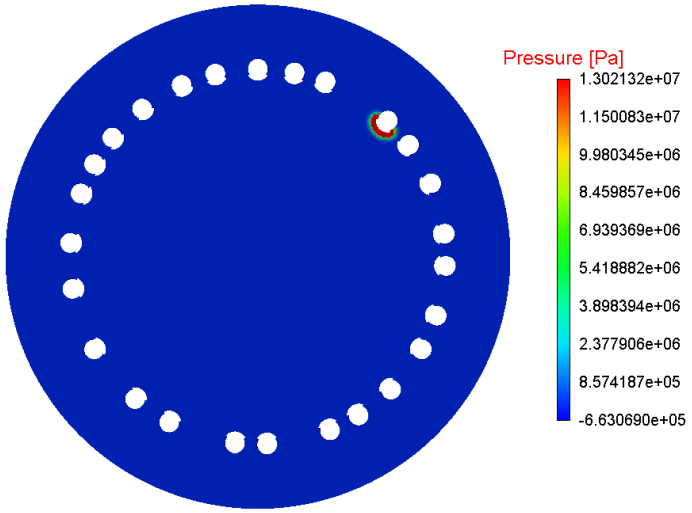

0,00004 s

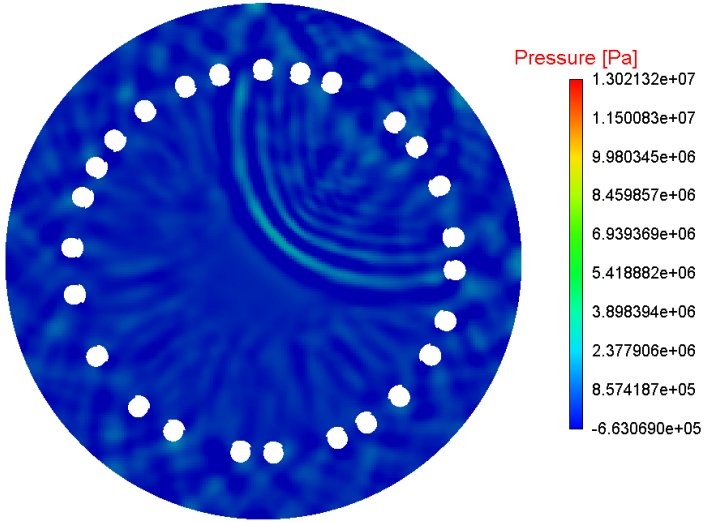

0,00016 s

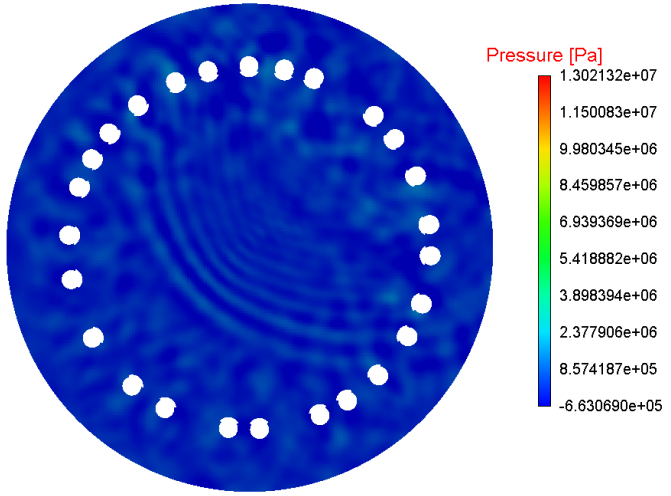

0,00023 s

Speeding up the solution of the inverse problem. Optimization

Tumor detection with a resolution of ≈ 1 mm (500 x 500 x 500) ≈ 4 TB is required to store dynamic direct problem (double) data.

- Maximize the use of a priori information to reduce memory storage requirements.
- Supercomputer: $\boldsymbol{T_{\mathrm{IP}} := T_{\mathrm{DP}} \times 4 \times N_{\mathrm{sources}} \times N_{\mathrm{iterations}}}$.
- Direct problems solve on a separate computing node to calculate the gradient for each source $\boldsymbol{T_{\mathrm{IP}} := T_{\mathrm{DP}} \times 4 \times N_{\mathrm{iterations}}}$.
- Stochastic gradients: $\boldsymbol{N_{\mathrm{iterations}} := N_{\mathrm{iterations}}/2}$.
- NN/ML – good initial guess: $\boldsymbol{N_{\mathrm{iterations}} := N_{\mathrm{iterations}}/10}$.
- Supercomputer max: $\boldsymbol{T_{\mathrm{IP}} := T_{\mathrm{DP}} \times N_{\mathrm{iterations}}/5}$.
- Inverse problem in the frequency domain.

Conclusion

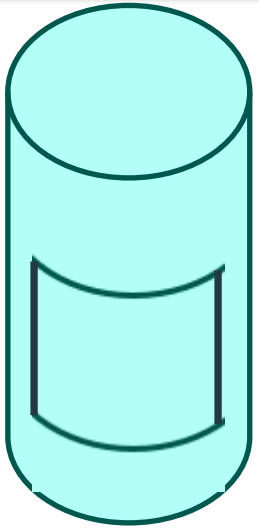

Sources/receivers: diameter 2 cm, height 5 cm.

Antenna: 1 cm source/receiver, 3 cm height.

Averaging the signal over the receiver area!

2d: 8 sources/receivers (500 x 500) – 56 curves, 15,000 datasets – **74 hours** (50 + 24).

3d: 256 sources/receivers x 50 slices (120 x 120 x 120) – 65280 x 50 Number of slices ≈ 250,000,000 datasets

≈ **2000 days** on a HPC workstation for datasets preparing and ML.

≈ **60 days** on a supercomputer Sergey Godunov (Sobolev Institute of Mathematics 120 TFlops).

Thank you for your time!

References

- Klingenberg C and Risebro N H 1995 Convex conservation laws with discontinuous coeffcients. Existence, uniqueness and asymptotic behavior Comm. Partial Diff. Eqns 20 1995, 90.
- Helge Holden, Fabio Simone Priuli, Nils Henrik Risebro. On an inverse problem for scalar conservation laws. Inverse Problems. 2014. Volume 30, Number 3
- I.M. Anderson, J. Pohjanpelto, Variational principles for differential equations with symmetries and conservation laws. I. Second order scalar
- equations, Math. Ann. 299 (1994) 191–222.
- I.M. Anderson, J. Pohjanpelto, Variational principles for differential equations with symmetries and conservation laws. II. Polynomial differential equations, Math. Ann. 301 (1995) 627–653.
- R.O. Popovych, A. Bihlo, Symmetry preserving parameterization schemes, J. Math. Phys. 53 (2012) 073102
- D.J. Stensrud, Parameterization Schemes: Keys to Understanding Numerical Weather Prediction Models, Cambridge University Press, Cambridge, 2007.
- A. Bihlo, E.M. Dos Santos Cardoso-Bihlo, R.O. Popovych, Invariant parameterization and turbulence modeling on the beta-plane, Physica D 269 (2014) 48–62,
- M. Oberlack, Invariant modeling in large-eddy simulation of turbulence, in: Annual Research Briefs, Stanford University, 1997.
- A. Bihlo, G. Bluman, Conservative parameterization schemes, J. Math. Phys. 54 (2013) 083101, arXiv:12094279.
- R.B. Stull, An Introduction to Boundary Layer Meteorology, in: Atmospheric Sciences Library, vol. 13, Kluwer Academic Publishers, Dortrecht, 1988.

References

- Burov, V.A.; Voloshinov, V.B.; Dmitriev, K.V.; Polikarpova, N.V. Acoustic waves in metamaterials, crystals, and anomalously refracting structures. Adv. Phys. Sci. **2011**, 54, 1165–1170.
- Burov, V.A.; Zotov, D.I.; Rumyantseva, O.D. Reconstruction of spatial distributions of sound velocity and absorption in soft biological tissues using model ultrasonic tomographic data. Acoust. Phys. **2014**, 60, 479–491.
- Burov, V.A.; Zotov, D.I.; Rumyantseva, O.D. Reconstruction of the sound velocity and absorption spatial distributions in soft biological tissue phantoms from experimental ultrasound tomography data. Acoust. Phys. **2015**, 61, 231–248.
- Duric, N.; Littrup, P.; Poulo, L.; Babkin, A.; Pevzner, R.; Holsapple, E.; Rama, O.; Glide, C. Detection of breast cancer with ultrasound tomography: First results with the computed ultrasound risk evaluation (CURE) prototype. Med. Phys. **2007**, 34, 773–785.
- Duric, N.; Littrup, P.; Li, C.; Roy, O.; Schmidt, S.; Janer, R.; Cheng, X.; Goll, J.; Rama, O.; Bey-Knight, L.; et al. Breast ultrasound tomography: Bridging the gap to clinical practice. Proc. SPIE **2012**, 8320, 83200O.
- Jirik, R.; Peterlik, I.; Ruiter, N.; Fousek, J.; Dapp, R.; Zapf, M.; Jan, J. Sound-Speed image reconstruction in sparse-aperture 3D ultrasound transmission tomography. IEEE Trans. Ultrason. Ferroelectr. Freq. Control **2012**, 59, 254–264.
- Wiskin, J.; Borup, D.; Andre, M.; Johnson, S.; Greenleaf, J.; Parisky, Y.; Klock, J. Three dimensional nonlinear inverse scattering: Quantitative transmission algorithms, refraction corrected reflection, scanner design, and clinical results. Proc. Meet. Acoust. **2013**, 19, 075001.
- Wiskin, J.; Borup, D.; Iuanow, E.; Klock, J.; Lenox, M. 3-D nonlinear acoustic inverse scattering: Algorithm and quantitative results. IEEE Trans. Ultrason. Ferroelectr. Freq. Control **2017**, 64, 1161–1174.
- Wiskin, J.; Malik, B.; Natesan, R.; Lenox, M. Quantitative assessment of breast density using transmission ultrasound tomography. Med. Phys. **2019**, 46, 2610–2620.
- Wiskin, J.;Malik, B.; Natesan, R.; Borup, D.; Pirshafiey, N.; Lenox,M.; Klock, J. FullWave 3D Inverse Scattering Transmission Ultrasound Tomography: Breast and Whole Body Imaging. In Proceedings of the IUS—IEEE International Ultrasonics Symposium, Glasgow, UK, 6–9 October 2019; pp. 951–958.
- Filatova, V.; Danilin, A.; Nosikova, V.; Pestov, L. Supercomputer Simulations of the Medical Ultrasound Tomography Problem. Commun. Comput. Inf. Sci. **2019**, 1063, 297–308.

References

- Beilina, L.; Klibanov, M.V. Synthesis of global convergence and adaptivity for a hyperbolic coefficient inverse problem in 3D. J. Inverse Ill-Posed Probl. **2010**, 18, 85–132.
- Klibanov, M.V. Travel time tomography with formally determined incomplete data in 3D. Inverse Probl. Imaging **2019**, 13, 1367–1393. Klibanov, M.V. On the travel time tomography problem in 3D. J. Inverse Ill-Posed Probl. **2019**, 27, 591–607.
- Kabanikhin, S.I.; Kulikov, I.M.; Shishlenin, M.A. An Algorithm for Recovering the Characteristics of the Initial State of Supernova. Comput. Math. Math. Phys. **2020**, 60, 1008–1016.
- Godunov, S.K. Differential method for numerical computation of noncontinuous solutions of hydrodynamics equations. Matematicheskiy Sbornik **1959**, 47, 271–306. (In Russian)
- Godunov, S.K.; Zabrodin, A.V.; Ivanov, M.Y.; Kraikov, A.N.; Prokopov, G.P. Numerical Solution for Multidimensional Problems of Gas Mechanics; Nauka: Moscow, Russia, 1976.
- Kaltenbacher, B.; Nikolic, V.; Thalhammer, M. Efficient time integration methods based on operator splitting and application to the Westervelt equation. IMA J. Numer. Anal. **2014**, 35, 1092–1124.
- Baev, A.V. Numerical Solution of the Inverse Scattering Problem for the Acoustic Equation in an Absorptive Layered Medium. Comput. Math. Model. **2018**, 29, 83–95.
- Baev, A.V. Imaging of Layered Media in Inverse Scattering Problems for an Acoustic Wave Equation. Math. Models Comput. Simul. **2016**, 8, 689–702.
- Belishev, M.I.; Ivanov, I.B.; Kubyshkin, I.V.; Semenov, V.S. Numerical testing in determination of sound speed from a part of boundary by the BC-method. J. Inverse Ill-Posed Probl. **2016**, 24, 59–180.
- Belishev, M.I.; Vakulenko, A.F. On characterization of inverse data in the boundary control method. Rendiconti dell'Istituto di Matematica dell'Universita di Trieste **2016**, 48, 49–77.

References

- He, S.; Kabanikhin, S.I. An optimization approach to a three-dimensional acoustic inverse problem in the time domain. J. Math. Phys. **1995**, 36, 4028–4043.
- Beilina, L.; Klibanov, M.V. A posteriori error estimates for the adaptivity technique for the Tikhonov functional and global convergence for a coefficient inverse problem. Inverse Probl. **2010**, 26, 045012.
- Xin, J.; Beilina, L.; Klibanov, M. Globally convergent numerical methods for some coefficient inverse problems. Comput. Sci. Eng. **2010**, 12, 64–76.
- Kabanikhin, S.I.; Klyuchinskiy, D.V.; Novikov, N.S.; Shishlenin, M.A. Numerics of acoustical 2D tomography based on the conservation laws. J. Inverse Ill-Posed Probl. **2020**, 28, 287–297.
- Romanov, V.G.; Kabanikhin, S.I. Inverse Problems for Maxwell's Equations; VSP: Utrecht, The Netherlands, 1994.
- A. V. Goncharsky and S. Y. Romanov, Iterative methods for solving coefficient inverse problems of wave tomography in models with attenuation, *Inverse Problems* **33** (2017), no. 2, Article ID 025003.
- A. V. Goncharsky, S. Y. Romanov and S. Y. Seryozhnikov, Inverse problems of 3D ultrasonic tomography with complete and incomplete range data, *Wave Motion* **51** (2014), no. 3, 389–404.
- A. V. Goncharsky, S. Y. Romanov and S. Y. Seryozhnikov, A computer simulation study of soft tissue characterization using low-frequency ultrasonic tomography, *Ultrasonics* **67** (2016), 136–150.
- S.J. Norton, M. Linzer, Ultrasonic reflectivity tomography: reconstruction with circular transducer arrays. Ultrason. Imaging, 1979, Vol. 2, pp. 154-184
- P. L. Karson, C.R. Meyer, A.L. Scherzinger, T.V. Oughton, Breast imaging in coronal planes with simultaneous pulse echo and transmission ultrasound. Science, 1981, Vol. 214, p. 1141-1143
- F. Natterer, F. Wubbeling, A pr opagation-backpropagation method for ultrasound tomography, Inverse problems, 1995, Vol. 11, p. 1225-1232
- F. Natterer, Reflectors in wave equation imaging. Wave motion, 2008, Vol. 45, p. 776-784.

Factorization of the inverse to the block-Toeplitz matrix

- Inverse A^{-1} to matrix A, in general, can be reconstructed by some subset of its elements $\{a_{ij}^{-1}\}$.

- Let A be the block-Toeplitz matrix, that consists of $n \times n$ blocks of $p \times p$ size. The following representation takes place[]:

$$A^{-1} = \begin{bmatrix} x_0 & 0 & \dots & 0 \\ x_1 & x_0 & \dots & 0 \\ \dots & \dots & \dots & \dots \\ x_{n-1} & x_{n-2} & \dots & x_0 \end{bmatrix} x_0^{-1} \begin{bmatrix} z_0 & z_1 & \dots & z_{n-1} \\ 0 & z_0 & \dots & z_{n-2} \\ \dots & \dots & \dots & \dots \\ 0 & 0 & \dots & z_0 \end{bmatrix} - \begin{bmatrix} 0 & 0 & \dots & 0 \\ y_0 & 0 & \dots & 0 \\ \dots & \dots & \dots & \dots \\ y_{n-2} & y_{n-3} & \dots & 0 \end{bmatrix} y_{n-1}^{-1} \begin{bmatrix} 0 & w_0 & \dots & w_{n-2} \\ 0 & 0 & \dots & w_{n-3} \\ \dots & \dots & \dots & \dots \\ 0 & 0 & \dots & 0 \end{bmatrix}$$

Here x_i, z_j, y_k, w_l - block components of block columns x, z and block rows y, w, such that

$$A \begin{bmatrix} x_0 & z_0 \\ \vdots & \vdots \\ x_{n-1} & z_{n-1} \end{bmatrix} = \begin{bmatrix} I & 0 \\ 0 & \vdots \\ \vdots & 0 \\ 0 & I \end{bmatrix}, \begin{bmatrix} y_0 & \cdots & y_{n-1} \\ w_0 & \cdots & w_{n-1} \end{bmatrix} A = \begin{bmatrix} I & 0 & \cdots & 0 \\ 0 & \cdots & 0 & I \end{bmatrix}$$

In other words, the inverse to block-Toeplitz matrix can be reconstructed by its first and last block row and block column.

Levinson-Durbin recursion

Let us consider the recursive procedure for computing the first and last block column of the inverse matrix A^{-1}.

Let us consider A_k - lead submatrix of block-Toeplitz matrix A: $A_0 = a_0, A_1 = \begin{pmatrix} a_0 & a_1 \\ a_{-1} & a_0 \end{pmatrix}, \dots A_{n-1} = A.$

Let us assume, that block columns x^k, z^k, such that $A_k[x^k\ z^k] = \begin{bmatrix} I & 0 \\ \dots & \dots \\ 0 & I \end{bmatrix}$, are known. The goal is to obtain x^{k+1}, z^{k+1}.

Using the properties of x^k, the following ratio can be written:

$$A_{k+1}\begin{bmatrix} x^k \\ 0 \end{bmatrix} = \begin{bmatrix} & A_k & & a_{k+1} \\ & & & a_k \\ & & & \dots \\ a_{-k+1} & a_{-k} & \dots & a_0 \end{bmatrix}\begin{bmatrix} x^k \\ 0 \end{bmatrix} = \begin{bmatrix} 1 \\ 0 \\ \\ \dots \\ 0 \\ \epsilon_x^n \end{bmatrix}$$

Here the error $\epsilon_x^n = a_{-k+1}x_0^k + \dots + a_{-1}x_{k-1}^k$. The identic ratio for z^k can be obtained:

$$A_{k+1}\begin{bmatrix} 0 \\ z^k \end{bmatrix} = \begin{bmatrix} a_0 & a_1 & \dots & a_{k+1} \\ a_{-1} & & & \\ \dots & & A_k & \\ a_{-k+1} & & & \end{bmatrix}\begin{bmatrix} 0 \\ z^k \end{bmatrix} = \begin{bmatrix} \epsilon_z^n \\ 0 \\ \\ \dots \\ 0 \\ 1 \end{bmatrix}$$

The idea is to find linear combination of $\begin{bmatrix} x^k \\ 0 \end{bmatrix}$ and $\begin{bmatrix} 0 \\ z^k \end{bmatrix}$ to eliminate ϵ_x^n and ϵ_z^n in the right part of equations.

Levinson-Durbin recursion

Let us find the linear combination, such, that

$$x^{k+1} = \alpha_x^n \begin{bmatrix} x^k \\ 0 \end{bmatrix} + \beta_x^n \begin{bmatrix} 0 \\ z^k \end{bmatrix}, z^{k+1} = \alpha_z^n \begin{bmatrix} x^k \\ 0 \end{bmatrix} + \beta_z^n \begin{bmatrix} 0 \\ z^k \end{bmatrix}$$

The coefficients $\alpha_x^n, \alpha_z^n, \beta_x^n, \beta_z^n$ can be defined by using the property

$$A_{k+1}[x^{k+1}\ z^{k+1}] = \begin{bmatrix} I & 0 \\ \dots & \dots \\ 0 & I \end{bmatrix}$$

The following system can be obtained:

$$\begin{bmatrix} I & \epsilon_x^n \\ \epsilon_z^n & I \end{bmatrix} \begin{bmatrix} \alpha_x^n & \alpha_z^n \\ \beta_x^n & \beta_z^n \end{bmatrix} = \begin{bmatrix} I & 0 \\ 0 & I \end{bmatrix}$$

This system has an unique solution, when the matrix A is non-singular.

Solving of this system allows to make step $x^k, z^k \to x^{k+1}, z^{k+1}$.

Therefore, the considered recursive procedure allows to compute the sequence of block columns

$$x^0 = z^0 = a_0^{-1} \to x^1, z^1 \to \dots \to x^{n-1} = x, z^{n-1} = z.$$

The recursive procedure for computing first and last block rows y, w can be written in the same manner.

Solving the system of linear algebraic equations

Usually, the inverse matrix A^{-1} is used for solving linear system with multiple right parts. When the solution is required for only one specific system $Aq = f$, the Levinson-Durbin recursive procedure can be adjusted for solving such system.

For every $k = 0, \dots, n-1$ we consider the system $A_k q^k = f^k$, where $f^k = \begin{bmatrix} f_0 \\ f_1 \\ \dots \\ f_{k-1} \end{bmatrix}$. Then $f^{n-1} = f$, $q^{n-1} = q$.

Then we can obtain:

$$A^k \begin{bmatrix} q_0^{k-1} \\ \dots \\ q_{k-1}^{k-1} \\ 0 \end{bmatrix} = \begin{bmatrix} f_0^{k-1} \\ \dots \\ f_{n-1}^{k-1} \\ \epsilon_q^{k-1} \end{bmatrix}$$

Here ϵ_q^{k-1} can be calculated in the same manner, as ϵ_x, ϵ_z earlier. Then this error can be eliminated and q^k can be computed:

$$\mathrm{q}^{\mathrm{k}} = \begin{bmatrix} q_0^k \\ \dots \\ q_{k-1}^k \\ q_k^k \end{bmatrix} = \begin{bmatrix} q_0^{k-1} \\ \dots \\ q_{k-1}^{k-1} \\ 0 \end{bmatrix} + \left(f_k - \epsilon_q^k\right) z^k$$

The GLK-equation for $x = L$ is solved by this method, the recursion allows us to find the solution of all GLK-equations for $x < L$.